INVESTIGATION OF Mg AND Sr DISTRIBUTION IN SPELEOTHEM

INVESTIGATION OF Mg AND Sr DISTRIBUTION IN SPELEOTHEM

By

JUDITH A. JOHNSON

Submitted to the Department of Geology
in Partial Fulfilment of the
Requirements for the Degree
Honours Bachelor of Science

McMaster University

April, 1979

BACHELOR OF SCIENCE (1979) McMASTER UNIVERSITY

(GEOLOGY) HAMILTON, ONTARIO

TITLE: Investigation of Mg and Sr Distribution in Speleothem

AUTHOR: Judith A. Johnson

SUPERVISOR: Dr. Henry P. Schwarcz

NUMBER OF PAGES: i-vii;1-138

ABSTRACT

The distribution of Mg and Sr in speleothem from Yorkshire, England, Vancouver Island and West Virginia, was investigated. Concentrations of Mg range from 300 to greater than 3000 parts per million. Concentrations of Sr range from less than 100 to a few hundred parts per million. Sr partitioning between seepage water and calcite may be more rate sensitive than Mg partitioning.

It is possible that Mg and Sr in speleothem could provide information on kinetics and mechanism of speleothem formation and on seepage water and source rock composition.

It may be possible to interpret Mg concentration in speleothem in terms of temperature if equilibrium partitioning of Mg between calcite and seepage waters can be demonstrated.

ACKNOWLEDGEMENTS

Thanks are due to Mr. M. Gascoyne who initially suggested this topic and who has shown an interest in it throughout, to Dr. H.P. Schwarcz who has provided support, guidance and much useful advice during this project, to Ada Dixon and M. Mureika for their help in the laboratory - particularly in dating speleothem. Thin section preparation was carried out by Mr. L. Zwicker. Mr. Jack Whorwood provided assistance with photography.

My thanks to Helen Elliott for her calm professionalism in preparation of this manuscript, to Pamela Burns, Charles Yonge and Suzan Laidlaw for moral support.

I would like to thank Bob Bignell for his cheerful assistance in the field.

TABLE OF CONTENTS

ABBREVIATIONS AND SYMBOLS

ppm parts per million

TE trace element

λ_i partition coefficient of i between $CaCO_3$ and liquid

λ_i^c partition coefficient of i between calcite and liquid

λ_i^A partition coefficient of i between aragonite and liquid

m molality

[X] concentration of X ($\simeq$ activity)

$[X]_s$ concentration of X in solid

$[X]_\ell$ concentration of X in liquid

δ isotopic composition referred to standard Pee Dee formation Belemnite.

e.g.

$$\delta^{18}O_{PDB} = \frac{(^{18}O/^{16}O)_c - (^{18}O/^{16}O)_{standard}}{(^{18}O/^{16}O)_{standard}}$$

α isotopic fractionation factor.

e.g.

$$\alpha_{c-\ell} = \frac{\delta_c + 1000}{\delta_\ell + 1000}$$

λ' apparent partition coefficient, i.e. 'partition coefficient' for non-equilibrium deposits. As equilibrium is approached $\lambda' \rightarrow \lambda$.

CHAPTER I

INTRODUCTION

The term speleothem refers to $CaCO_3$ deposits which form in air filled cave passage. Seepage waters percolating through limestone acquire dissolved $CaCO_3$. Degassing of CO_2 and/or evaporation of water decreases $CaCO_3$ solubility when seepage waters enter the cave atmosphere. Precipitation of calcite and/or aragonite speleothem occurs as a result.

Formation of speleothem is an extremely slow process. The deposits studied grew at rates of 0.1-8.9 cm/Ka. Periods of growth often cover tens of thousands of years. Speleothem are relatively easy to date using U-series dating techniques, in many cases an internal stratigraphy is discernible. These features make speleothem attractive targets for paleo-environmental studies.

Isotopic composition has been studied and $\delta^{18}O$ used as a paleotemperature indicator (Gascoyne et al., 1978). A preliminary study was made with the intention of establishing whether magnesium concentration could also be used as a

paleothermometer.

Before discussing the aims and objectives of this study a brief review of terminology and mechanism of speleothem formation, including some discussion of isotopic and trace element partitioning between speleothem and parent seepage water, is presented.

Terminology

Speleothem varies in size and shape depending on the site of formation and the supply of seepage water. Various terms are applied to different formations. Soda straws form on the cave roof as water enters the cave. These formations have a central hole and are often extremely fragile. The central hole may become plugged with $CaCO_3$. Water then flows over the outside and deposits layers of $CaCO_3$ building a stalactite. Water falling to the cave floor precipitates $CaCO_3$ on formations termed stalagmites. These vary considerably in size and shape, layers of $CaCO_3$ often thin away from the point of impact of falling seepage water creating tall cylindrical stalagmites. Where large quantities of seepage water enter at one point flowstones may form. Sheets of $CaCO_3$ thin away from the source creating 'delta lobes'.

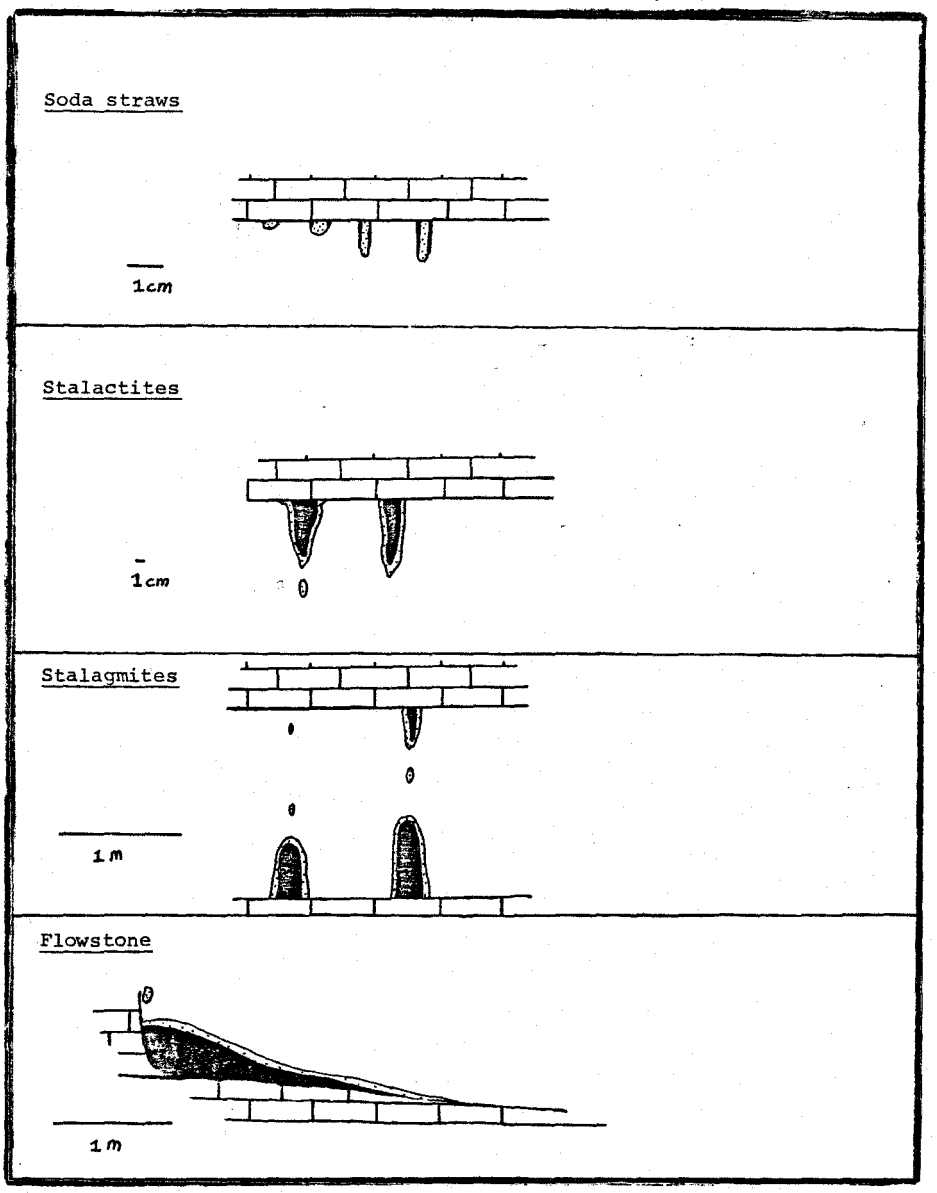

Types of Speleothem

seepage water

$CaCO_3$

Scales are approximate (size is variable)

Synchronously precipitated sheets of $CaCO_3$ are termed growth layers

Speleothem formation

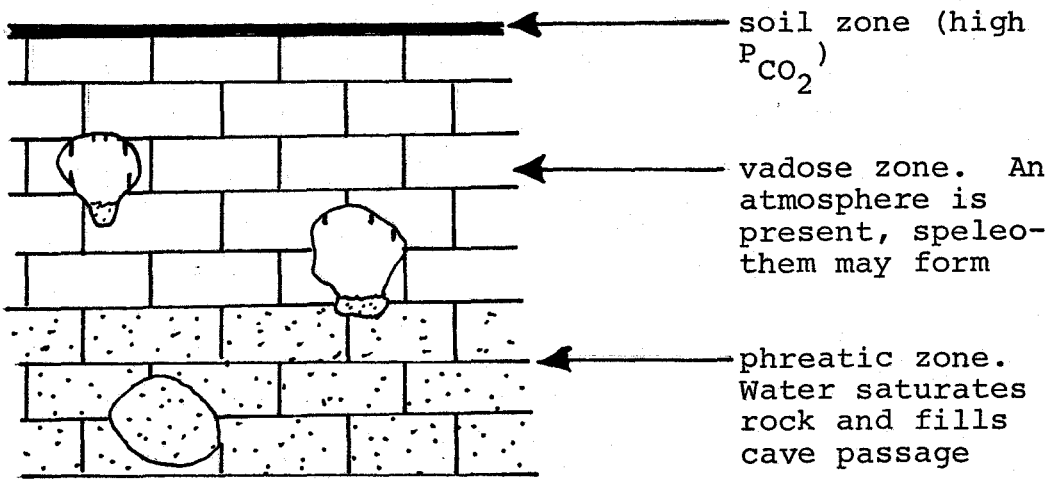

Mechanism of Precipitation of Speleothem. Definition of Partition Coefficients

Ground water obtains a P_{CO_2} above atmospheric levels in the soil zone. This results in the solution of considerable $CaCO_3$ in limestone karst areas. The major reactions involved are as follows:

$$H_2O + CO_2 \rightleftharpoons H_2CO_3$$
$$H_2CO_3 \rightleftharpoons H^+ + HCO_3^-$$
$$HCO_3^- \rightleftharpoons H^+ + CO_3^{2-}$$
$$CaCO_3 \rightleftharpoons Ca^{2+} + CO_3^{2-}$$

Holland et al. (1964b) give a detailed account of limestone and dolomite solution in systems with an extensive vadose zone (open systems) and systems where the ground water is not open to the air (closed systems). Maximum [Ca] in seepage water results when there is an extensive vadose zone and CO_2 from the atmosphere may continually replace that consumed by $CaCO_3$ solution.

When seepage waters enter the cave atmosphere $P_{CO_{2water}}$ will equilibrate with $P_{CO_{2atmosphere}}$. This reduces the solubility of $CaCO_3$ and results in calcite or aragonite precipitation. Evaporation of water also decreases the solubility of $CaCO_3$ contributing to calcite precipitation. Holland et al. have shown that at least in the deep cave environment evaporation is negligible. Humidity in deep caves is often 100%. This was checked by the author in two caves in West Virginia (Friars Hole and Norman-Bone in the west section). An air temperature was obtained using a dry thermometer - a wet cloth was then wrapped around the thermometer bulb, the thermometer was swung to and fro rapidly for several minutes, the temperature was taken again immediately. No change was detected. (The thermometer was calibrated to 0.1°C).

Evaporation and/or degassing at low rates would allow precipitation of calcite with equilibrium trace element

concentrations. Partly evaporative speleothem has been demonstrated in the modern cave environment, e.g. in Carlsbad caverns (Thrailkill, 1971).

Degassing of CO_2 enriches the liquid phase in ^{14}C and ^{13}C with respect to ^{12}C. Evaporation causes enrichment of ^{18}O in the liquid phase with respect to ^{16}O. This becomes important when correlation of $\delta^{18}O$, $\delta^{13}C$, [Sr] and [Mg] are considered.

The partition coefficient for trace element partitioning between water and calcite is defined as follows:

$$\lambda^{C}_{TE} = \frac{[TE]_s [Ca]_L}{[Ca]_s [TE]_L}$$

The value of λ^{C}_{TE} applies to precipitation of a homogeneous crystal in equilibrium with the liquid, or to a zoned crystal where surface equilibrium is maintained. Calculations in this paper assume surface equilibrium (logarithmic distribution).

In laboratory investigations reported in the literature the most reliable results have been obtained assuming logarithmic distribution. (See compilation of values of λ^{C}_{Sr} and λ^{C}_{Mg} pp. and for references). The partition coefficient

λ_{TE} only applies where the relation between TE:Ca ratio is linear, i.e. at low $[TE]_L$. It is not known at what point λ^c_{Mg} or λ^c_{Sr} cease to apply.

The isotopic fractionation factor α is defined as

$$\alpha_{c-\ell} = \frac{\delta_c + 1000}{\delta_\ell + 1000}$$

where δ_c = isotopic composition of calcite;

δ_ℓ = isotopic composition of seepage water.

α is temperature dependent. Thus δ_c depends on temperature and liquid composition. Values of α appreciably different from 1 are found only for light elements. In this case fractionation of stable isotopes of C and O between water and speleothem is measurable. In non-evaporative speleothem the isotopic composition of the water remains constant as $CaCO_3$ is precipitated. Thus oxygen isotopic composition of $CaCO_3$ is a function of seepage water composition and of temperature. C isotopic composition will also be a function of the amount of degassing which has occurred.

Aims and objectives of this project

The original objective of this project was to compare [Mg] and $\delta^{18}O$ in speleothem - both quantities which are known to be temperature dependent. The project was initiated following the recognition of temperature dependence of Mg partitioning between dilute aqueous solutions and calcite. Temperature dependence for equilibrium partitioning determined in the laboratory (Katz, 1973) led to investigation in the field. Partition coefficients were determined for several actively growing soda straws in caves in Jamaica and Vancouver Island. The results showed a strong temperature dependence but disagreed with previous laboratory determinations of equilibrium partition coefficients (Gascoyne, 1979).

Water which is continuously depositing relatively pure calcite is continuously increasing its TE:Ca ratio. It is therefore impossible to use [Mg] in isolation as a temperature indicator. Sr was known to be present in many speleothem deposits in detectable quantities; it had recently been shown that equilibrium partitioning of Sr between calcite and water was temperature independent (Katz et al.,

1972). It was decided that the two elements should be studied together.

Results are presented for several deposits from Yorkshire, England and for two speleothem for which Mg, Sr, $\delta^{18}O$ and $\delta^{13}C$ determinations have been made.

This study has concentrated on calcite speleothem. Since λ^{A}_{Sr} is temperature sensitive a similar study could have been made using aragonite speleothem. Aragonite precipitation is favoured by high temperatures and high $[Mg]_L$, while calcite is favoured at lower temperatures and $[Mg]_L$ (e.g. Murray, 1954; Moore, 1956; Kitano, 1962). The mineralogy of speleothem is easily determined by visual inspection. However, traces of aragonite in calcite are not easily detected. Mineralogy was confirmed using a chemical test (Feigls solution). Results should also be checked using X-ray diffraction.

CHAPTER II

THEORETICAL CONSIDERATIONS

Equilibrium Values of Partition Coefficients

Equilibrium values of λ^{c}_{TE} for Mg and Sr obtained by Katz (1973; Katz et al., 1972), using inversion of pure aragonite to calcite in the presence of an aqueous medium containing the TE in question, appear to be the most reliable. Higher values for λ^{c}_{Sr} obtained at low temperatures in direct precipitation experiments may be due to rapid precipitation, if surface equilibrium is not maintained when an apparent partition coefficient $\lambda^{c'}_{TE}$ will be obtained rather than the true logarithmic partition coefficient λ^{c}_{TE}. Sr appears to be far more sensitive to kinetic effects than Mg (see Kinetic Effects, p.14).

If Katz's results are correct then λ^{c}_{Mg} increases linearly with temperature and λ^{c}_{Sr} is virtually independent of temperature. Various determinations of λ_{Mg} and λ_{Sr} have been compiled and graphed.

λ^{c}_{Mg} - temperature dependence

Reference	Method	Comments	T°C	λ^{c}_{Mg}
Katz, 1973	Inversion of aragonite to calcite	High values noted for rapid inversion	25	0.0573± 0.0017
			35	0.0681± 0.0019
			50	0.0778± 0.0022
			70	0.0973± 0.0021
			90	0.1163± 0.0034
Gascoyne, 1979	Measurement of seepage waters and growing soda straws	Vancouver Island 5 determinations	7	∿0.02
		Jamaica 7 determinations	22-24	∿0.04

λ^{c}_{Sr} - compilation of reported values

Reference	Method	Comment	T°C	λ^{c}_{Sr}
Katz et al., 1972	Inversion of aragonite to calcite		40 98	0.055 0.058
Holland et al., 1964a	Degassing of CO_2 from ammoniacle $CaCl_2$ solution at high P_{CO_2}	Independent of ionic strength to 1.4 M	100	0.076± 0.006
Holland et al., 1964b	Measurement of Ca and Sr in cave waters and calcite precipitates	High values attributed to calcite precipitation from earlier Sr rich waters	16.4 14.4 15	0.14±0.03 0.22±0.06 0.13±0.06
Kitano et al., 1971	Degassing (of CO_2)	Independent of Mg concentration	20	0.08±0.02
Joshi, 1960 Holland, 1960	Experimental result		25	0.14±0.02

Note that if values determined by Kitano and Holland at low temperatures are correct, then λ^{c}_{Sr} decreases with temperature

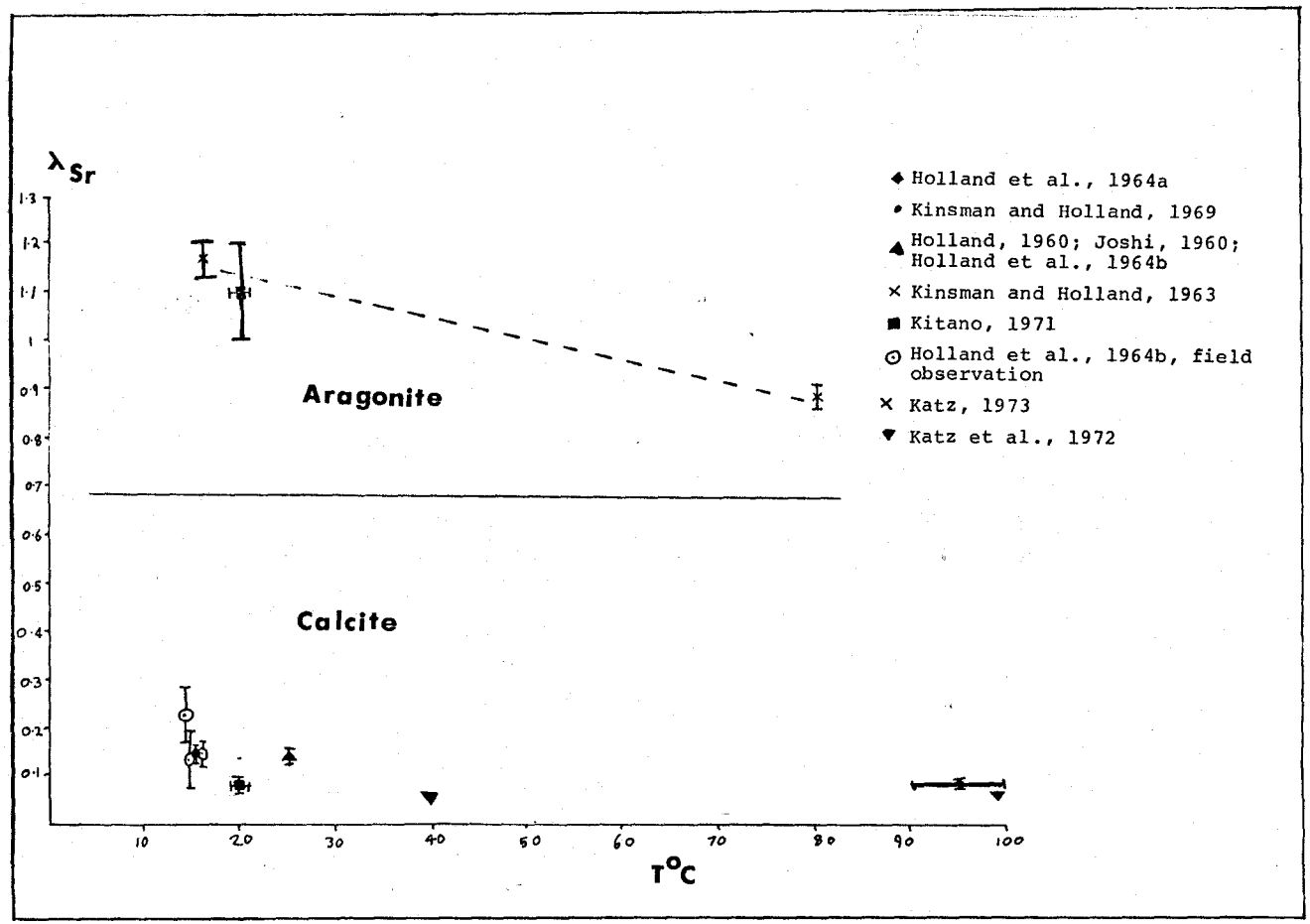

Partition Coefficients for Sr

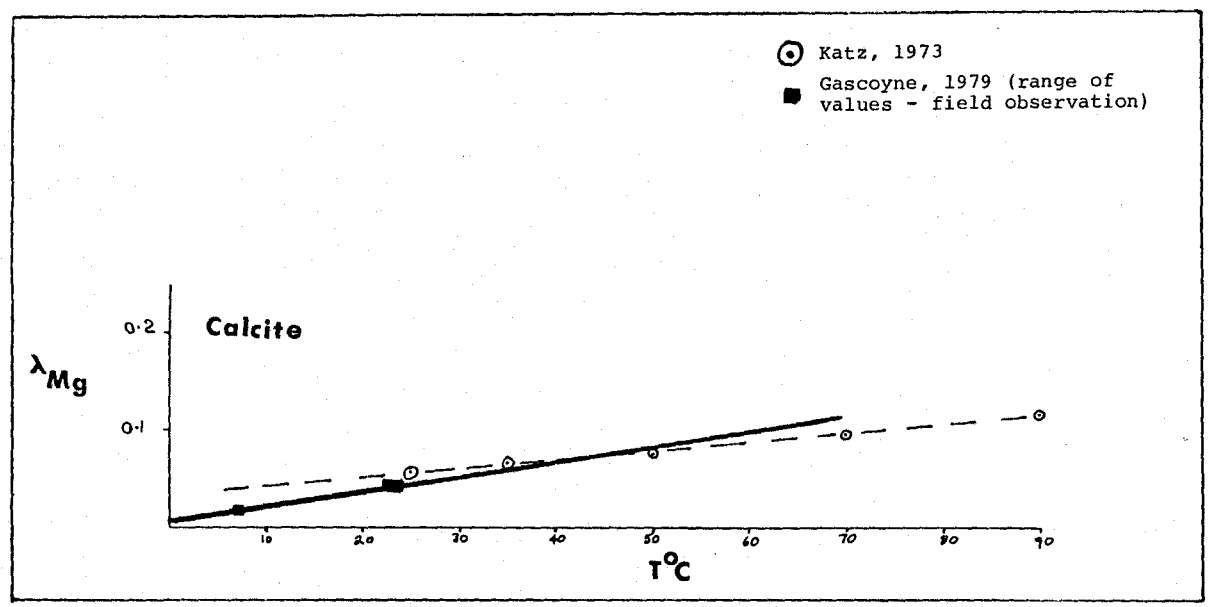

Partition Coefficients for Mg

Kinetic Effects. Deviation of λ^c_{TE} from Equilibrium Values

If Katz's results for λ^c_{Mg} and λ^c_{Sr} are accepted as true equilibrium values then earlier results must be explained in terms of disequilibrium phenomena.

High values for λ^c_{Sr} in early stages of calcite precipitation were obtained by Kitano et al. (1971). Abnormally high values of λ^c were easily obtained by them for metals forming carbonates with the aragonite crystal form (Ba and Sr). High values were not so easily obtained for metals forming carbonates with the calcite crystal from (Cu, Zn). Abnormally high values were attributed by Kitano to abnormal crystal structure of fine early precipitates. However X-ray diffraction patterns were obtained for late stage precipitates only. $\lambda^{c'}$ was determined using samples of the supernatent solution withdrawn during the precipitation process. Kitano took the final ($\sim$ constant) values of λ^c as the equilibrium value. The Doerner-Hoskins relation was used to calculate $\lambda^{c'}$ and λ^c. Clear X-ray diffraction patterns of large late stage crystalline precipitates indicates that if early stage fine precipitates had an abnormal structure then they recrystallised. Kitano's value for λ^c_{Sr} is 0.08 ± 0.02; this value is higher than that obtained by aragonite-calcite transformation (Katz et al., 1972).

If one accepts that λ^C is virtually temperature independent with a value of about 0.055, then Kitano's result may be explained by the presence of a Sr-rich core in the final calcite crystals. A similar explanation might account for similar λ^C_{Sr} values obtained by Holland *et al.* (1964a). We have:

$$\lambda^C_{Sr} = \frac{\ell n \, [Sr]_{Li} \, / \, [Sr]_{Lf}}{\ell n \, [Ca]_{Li} \, / \, [Ca]_{Lf}} \qquad \text{(Doerner Hoskins relation)}$$

for equilibrium precipitation.

Abnormally high values of λ^C_{Sr} in the early stages of crystallisation would cause a decrease in $[Sr]_{Lf}$ with respect to the equilibrium value. This increases calculated λ^C_{Sr} over the true equilibrium value.

The fact that high values of λ^C_{TE} were less easily obtained for elements forming carbonates with the calcite crystal form suggests that Mg is less sensitive than Sr to kinetic effects.

Field measurements of λ^C_{Mg} (Gascoyne, 1979) gave values below those obtained by aragonite-calcite inversion (Katz, 1973). There are several possible explanations for this:

(1) Values obtained by aragonite-calcite inversion may be in excess of the true equilibrium value.

(2) Values measured in the field may be below the true equilibrium value because of kinetic effects.

(3) Values of $[TE]_{Lf}$ measured in the field may be in error. Since precipitation of speleothem occurs at extremely low rates the value of $[TE]_{Lf}$ measured over a short period of time may not coincide with $[TE]_{Lf}$ during precipitation of the calcite analysed.

(4) Relation to temperature might be non-linear (Gascoyne's determinations were at lower temperatures than Katz's).

The second explanation seems unlikely. High values of λ^{c}_{Mg} were obtained by Katz for rapid inversion of aragonite to calcite.

Field measurements of λ^{c}_{Sr} (Holland et al., 1964b) resulted in a range of values from 0.13 to 0.22. Joshi's determination of λ^{c}_{Sr} at 25°C was used to explain the low values (λ^{c}_{Sr} = 0.14 at 25°C, Joshi, 1960). High values were attributed to precipitation from earlier Sr-rich waters.

It seems likely that high values of λ^{c}_{Sr} recorded in the field are due at least in part to rapid precipitation and disequilibrium.

Kinetic effects on λ are discussed by McIntire (1963).

For uniform supersaturation the equation

$$\lambda^{c'} = \frac{\lambda^{c} S \, \delta_{TE}/\delta_{Ca}}{\lambda^{c}(S-1) + \delta_{TE}/\delta_{Ca}}$$

where $S = [Ca]_L/[Ca]_f$ (degree of supersaturation)

δ = diffusion coefficient

$[Ca]_f$ = [Ca] for the case where the liquid has equilibrated with calcite at that P_{CO_2}

may be applied.

For $\lambda^{c} < \delta_{TE}/\delta_{Ca}$, $\lambda^{c'}$ decreases with decreasing S. For TEs with ions of similar charge and radius to Ca $\delta_{TE}/\delta_{Ca} \simeq 1$.

For Sr and Mg we can expect values of $\lambda^{c'} > \lambda^{c}$ for supersaturated solutions.

Climatic Effects on Trace Element Content of Equilibrium Speleothem

There are three possible causes of variation in Mg/Sr, Mg/Ca and Sr/Ca ratios in seepage waters:

(1) Change in catchment area for water flowing over a particular deposit.

(2) Changes in P_{CO_2} causing variable solubility of limestone and dolomite. (Only significant where dolomite is present with limestone in the area.)

(3) Back equilibration of ground water and rock. (This will cause a temperature dependence for $[Mg]_{Li}$.)

P_{CO_2} in the soil atmosphere depends on the extent of biological activity in the soil. This is controlled by climate. Minimum F_{Ca} will result from maximum P_{CO_2}. Thus maximum fractionation of trace elements and maximum deposition of speleothem will coincide with periods of maximum P_{CO_2}.

Back equilibration of water with rock would cause Mg:Sr ratio in seepage waters to increase with temperature.

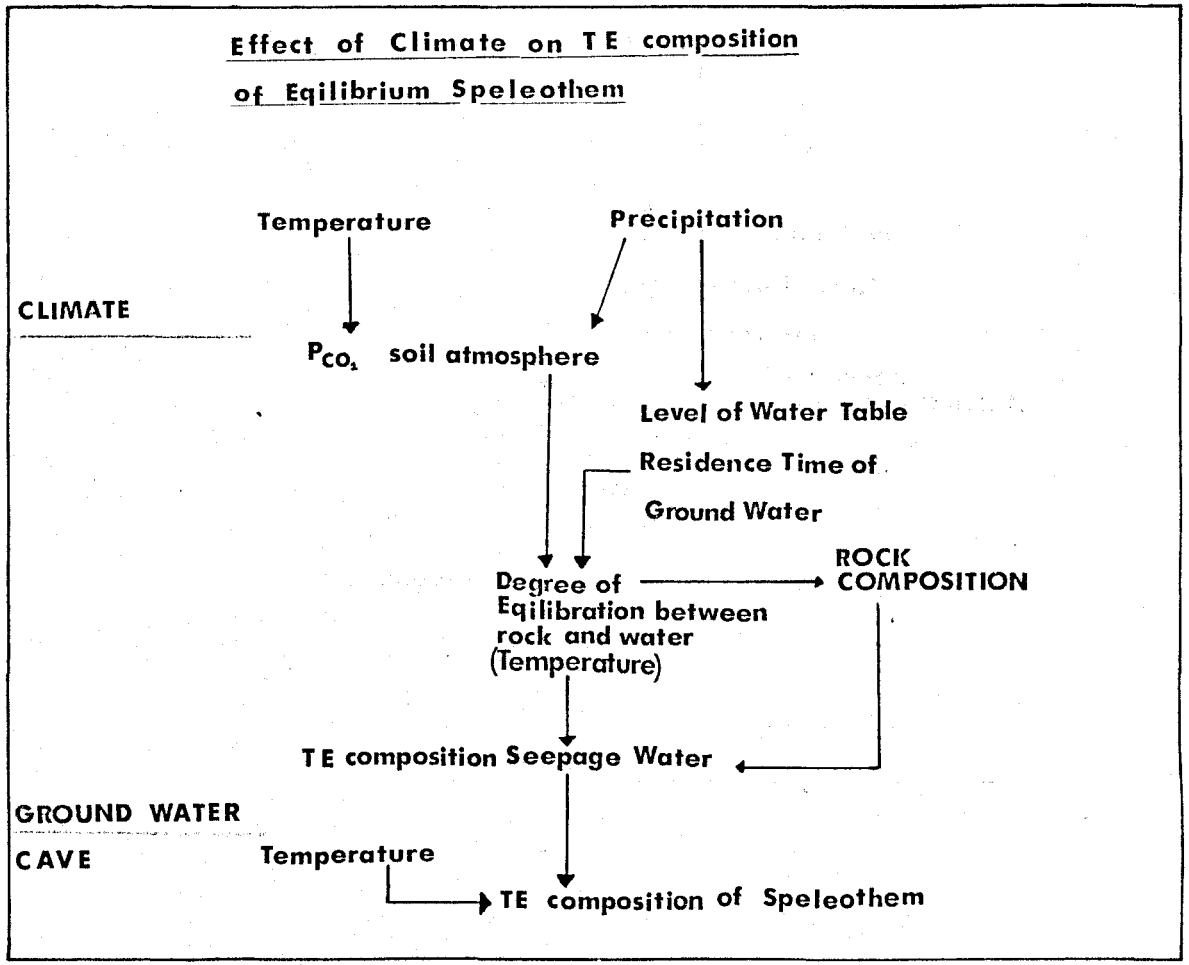
Effect of Climate on T E composition
of Eqilibrium Speleothem
Temperature
Precipitation
CLIMATE
P_{CO_2} soil atmosphere
Level of Water Table
Residence Time of
Ground Water
ROCK
COMPOSITION
Degree of
Eqilibration between
rock and water
(Temperature)
T E composition Seepage Water
GROUND WATER
CAVE
Temperature
TE composition of Speleothem

Equilibration need not be complete for a temperature effect to occur. However back equilibration seems unlikely. The logarithmic distribution law is followed for Mg distribution in precipitation of calcite (Katz, 1973). This suggests that solid state diffusion leading to equilibration between water and rock is an immeasurably slow process.

Changes in catchment area for one deposit resulting from changes in ground water circulation routes are possible. There is no easy way to detect this - sudden changes in Mg/Sr ratio in speleothem, especially those following a break in deposition should be regarded with suspicion.

If bulk solution of the surrounding rock occurs then temperature changes resulting in change in λ^{c}_{Mg} will be recorded by changes in the Mg/Sr ratio of equilibrium speleothem.

The flow chart opposite summarises the possible climatic effects. The amount of change in $[Mg]_s$ due to temperature change is uncertain but could be as high as 100% in 15°C (using Gascoyne's values for λ^{c}_{Mg}).

Climatic effects on $\delta^{18}O$ of speleothem are complex since $\delta^{18}O_{water}$ and α may vary. A full discussion of $\delta^{18}O$ of speleothem is outside the scope of this study. Generally $\delta^{18}O$ appears to increase with temperature (Gascoyne et al., 1978).

Derivation of Formulae for Equilibrium Speleothem Deposition

If we assume that instantaneous equilibrium between crystal surface and liquid is maintained during precipitation then we may apply the Doerner-Hoskins relation:

$$\frac{[TE]_s}{[Ca]_s} = \lambda_{TE} \frac{[TE]_L}{[Ca]_L} \quad \text{at any point.}$$

For precipitation of an infinitesimally thin layer of calcite:

$$\frac{dnTE_s}{dnCa_s} = \lambda_{TE} \left(\frac{nTE_{Li} - nTE_{sf}}{nCa_{Li} - nCa_{sf}}\right)$$

where n = number of moles

i = initial value

f = final value

$$\int_i^f \frac{dnTE_s}{nTE_{Li} - nTE_s} = \lambda_{TE} \int_i^f \frac{dnCa_s}{nCa_{Li} - nCa_s}$$

$$\ln \frac{[TE]_{Li}}{[TE]_{Lf}} = \lambda_{TE} \ln \frac{[Ca]_{Li}}{[Ca]_{Lf}}$$

Thus

$$\log \frac{1}{F_{TE}} = \lambda_{TE} \log \left(\frac{1}{F_{Ca}}\right)$$

where

$$F_{TE} = \frac{[TE]_{Lf}}{[TE]_{Li}}$$

We have:

(1) $$F_{Sr} = F_{Ca}^{\lambda_{Sr}} = \frac{[Sr]_{Lf}}{[Sr]_{Li}}$$

(2) $$F_{Mg} = F_{Ca}^{\lambda_{Mg}} = \frac{[Mg]_{Lf}}{[Mg]_{Li}}$$

In one growth layer the final value of (F_{Ca}) will depend on the initial conditions.

High P_{CO_2} and [Ca] of seepage waters leads to low (F_{Ca}) as the water equilibrates with the cave atmosphere. Analyses of cave waters at various stages of evolution gave a range of values from 0.6-2.7 m mol/l (Holland et al., 1964a). A minimum value of (F_{Ca}) of 0.2 is used in the following calculations. We know that λ_{Mg} and λ_{Sr} fall in the range 0.1-0.01. Calculated F_{TE} for F_{Ca} = 0.2 shows that very little change would be expected to occur in $[Sr]_{\ell}$ or $[Mg]_{\ell}$ along a growth layer.

Values of F_{TE} for Various F_{Ca} and λ_{TE}

F_{Ca}	$\lambda = 0.1$	$\lambda = 0.05$	$\lambda = 0.01$
0.1	0.794	0.891	0.977
0.2	0.851	0.922	0.984
0.5	0.933	0.966	0.993
0.9	0.989	0.995	0.999

From (1) and (2) we have

$$nSr_{Lf} = \left(\frac{1}{F_{Ca}}\right)^{-\lambda_{Sr}} nSr_{Li}$$

$$nMg_{Lf} = \left(\frac{1}{F_{Ca}}\right)^{-\lambda_{Mg}} nMg_{Li}$$

$$\rightarrow \quad \frac{[Mg]_{Lf}}{[Sr]_{Lf}} = \left(\frac{1}{F_{Ca}}\right)^{-\lambda_{Mg}+\lambda_{Sr}} \frac{[Mg]_{Li}}{[Sr]_{Li}}$$

i.e. smaller difference between λ_{Mg} and λ_{Sr} results in less fractionation between Mg and Sr in a growth layer.

We have:

$$0.05 < \lambda^{c}_{Sr} < 0.08 \quad (\lambda^{c}_{Sr} = \text{constant})$$

$$0.01 < \lambda^{c}_{Mg} < 0.10 \quad (\lambda^{c}_{Mg} \text{ T dependent})$$

$$\rightarrow \quad -0.02 < -\lambda^{c}_{Mg} + \lambda^{c}_{Sr} < 0.07$$

See compilation of values for λ^{c}_{Sr} and λ^{c}_{Mg} p. 11

for $F_{Ca} = 0.2$ this gives

$$\frac{[Mg]_{Lf}}{[Sr]_{Lf}} = K\frac{[Mg]_{Li}}{[Sr]_{Li}} \qquad \left(K = \left(\frac{1}{F_{Ca}}\right)^{-\lambda_{Mg}+\lambda_{Sr}}\right)$$

where:

$$0.968 < K < 1.12$$

i.e.

$$(3)\quad \frac{[Mg]_{Lf}}{[Sr]_{Lf}} = \frac{[Mg]_{Li}}{[Sr]_{Li}} \pm \begin{matrix} 16\% \\ 13\% \end{matrix}$$

) Including all temperature variation between 0 and 65°C and values of F_{Ca} greater than 0.2

Since λ^{c}_{Mg} is linearly temperature dependent we expect K to be linearly T dependent, $K = f(F_{Ca}, T)$. In one growth layer $K = f(F_{Ca})$, and

$$\frac{[Sr]_{si}}{[Ca]_{si}} = \lambda_{Sr}\frac{[Sr]_{Li}}{[Ca]_{Li}}$$

$$\frac{[Sr]_{sf}}{[Ca]_{sf}} = \lambda_{Sr}\frac{[Sr]_{Lf}}{[Ca]_{Lf}}$$

$$\frac{[Sr]_{si}}{[Sr]_{sf}} = \frac{[Sr]_{Li}}{[Sr]_{Lf}}\,\frac{[Ca]_{Lf}}{[Ca]_{Li}} = F_{Sr}^{-1}\,F_{Ca}$$

$$([Ca]_{sf} = [Ca]_{Si})$$

Similarly

$$\frac{[Mg]_{si}}{[Mg]_{sf}} = \frac{[Mg]_{Li}}{[Mg]_{Lf}} \frac{[Ca]_{Lf}}{[Ca]_{Li}} = F_{Mg}^{-1} F_{Ca}$$

If

$$F_{Sr} \sim F_{Mg} \sim 1 \text{ then } \frac{[Sr]_{si}}{[Sr]_{sf}} \simeq \frac{[Mg]_{si}}{[Mg]_{sf}} \simeq F_{Ca}$$

But

$$F_{Sr} = F_{Ca}^{\lambda_{Sr}}$$

Internal constancy may be checked. We may use estimated F_{Ca} to check for equilibrium λ_{Sr} or we may use λ_{Sr} to check our value for F_{Ca}.

F_{Ca} may be used to solve for λ_{Mg}, and hence for temperature:

$$F_{Mg} = F_{Ca}^{\lambda_{Mg}} = \frac{[Mg]_{Lf}}{[Mg]_{Li}} = \frac{[Mg]_{sf}}{[Mg]_{si}}$$

Comparing Different Growth Layers

If we consider seepage water produced by bulk solution of source rock of a fixed composition we may make the following statements.

$$\frac{[Mg]_{Li}}{[Sr]_{Li}} = c, \quad \frac{[Mg]_{Li}}{[Ca]_{Li}} = K_1, \quad \frac{[Sr]_{Li}}{[Ca]_{Li}} = K_2$$

But $$\frac{Sr_s}{Mg_s} = \frac{\lambda_{Sr}}{\lambda_{Mg}} \frac{[Sr]_L}{[Mg]_L}$$

and $$\log \frac{[Sr]_L}{[Sr]_{Li}} = -\lambda^c_{Sr} \log \frac{[Ca]_L}{[Ca]_{Li}}$$

Thus $$\frac{[Sr]_L}{[Sr]_{Li}} = \left(\frac{[Ca]_L}{[Ca]_{Li}} \right)^{-\lambda^c_{Sr}}$$

$$\rightarrow \quad \frac{[Sr]_L}{[Ca]_L} K_2^{-1} = \left(\frac{[Ca]_L}{[Ca]_{Li}} \right)^{-(\lambda^c_{Sr}+1)}$$

Similarly $$\frac{[Mg]_L}{[Ca]_L} K_1^{-1} = \left(\frac{[Ca]_L}{[Ca]_{Li}} \right)^{-(\lambda^c_{Mg}+1)}$$

$$\rightarrow \quad \frac{[Mg]_L}{[Sr]_L} \frac{K_2}{K_1} = F_{Ca}^{(\lambda^c_{Sr} - \lambda^c_{Mg})}$$

$$\rightarrow \quad \frac{[Mg]_L}{[Sr]_L} = cF_{Ca}^{(\lambda^c_{Sr} - \lambda^c_{Mg})}$$

$$\rightarrow \quad \frac{[Mg]_s}{[Sr]_s} = c \frac{\lambda^c_{Mg}}{\lambda^c_{Sr}} F_{Ca}^{(\lambda^c_{Sr} - \lambda^c_{Mg})}$$

Thus for a given $[Sr]_s$, $[Mg]_s$ is fixed provided λ^c_{Mg} and λ^c_{Sr} are constant.

But $[Mg]_s = f(T)$

and

$$\frac{[Mg]_s}{[Sr]_s} = \frac{\lambda^c_{Mg}}{\lambda^c_{Sr}} K \frac{[Mg]_L}{[Sr]_L}$$

Thus for points of given $[Sr]_s$ $[Mg]_s$ increases with temperature.

Disequilibrium Deposits

$\lambda^{c'}_{Mg}$ and $\lambda^{c'}_{Sr}$ may depart from the equilibrium values λ^{c}_{Mg} and λ^{c}_{Sr}. Variation of Mg:Sr ratios may exceed16% both within and between growth layers.

Field measurements and laboratory investigations have resulted in measurement of high values for $\lambda^{c'}_{Sr}$. Since $MgCO_3$ has the calcite crystal form we have a reason to suspect that variation in $\lambda^{c'}_{Sr}$ will exceed variation in $\lambda^{c'}_{Mg}$.

High supersaturation levels, rapid precipitation and disequilibrium are most likely to occur in waters with low F_{Ca} and low TE:Ca ratios.

Criteria for Equilibrium

In one growth layer of a stalagmite we see the evolution of the seepage water from high to low [Ca]. Since Mg:Ca and Sr:Ca ratios increase we expect to see an increase in [Mg] and in [Sr]. From equation (3) we see that we expect Mg:Sr ratio to change by less than 16% if equilibrium is maintained.

We may or may not see a change in $[Mg]_s$ and $[Sr]_s$ along a growth layer in a hand sample of flowstone. This will depend on whether or not a significant proportion of the Ca in solution was precipitated over that distance.

Since $F_{Mg} \sim F_{Sr}$ we expect a positive correlation of Mg and Sr between growth layers, provided Mg/Sr ratio in seepage waters is constant.

Criteria for isotopic equilibrium are given by Hendy (1971). In a deposit in isotopic equilibrium we expect constant $\delta^{18}O$ in one growth layer and no correlation of $\delta^{18}O$ with $\delta^{13}C$ in one growth layer.

Summary of Theoretical Considerations

Assuming bulk solution of limestone provides seepage waters with constant Mg/Sr, Mg/Ca and Sr/Ca ratios, we may distinguish between two extreme cases.

(1) Equilibrium deposition with variation in $[Mg]_s/[Sr]_s$ due to temperature. In this case variation in $[Mg]_s/[Sr]_s$ between growth layers should be chiefly due to $[Mg]_s$ variation. $[Mg]_s/[Sr]_s$ will be constant in one growth layer.

(2) Kinetic fractionation with variation in $[Mg]_s/[Sr]_s$ due to changes in saturation state. In this case $[Mg]_s/[Sr]_s$ variation may be due to $[Mg]_s$ or $[Sr]_s$ variation. $[Mg]_s/[Sr]_s$ will probably not be constant in one growth layer.

We should be able to detect kinetically fractionated deposits since these speleothem may show fluctuations of >16%* in Mg/Sr ratio in one growth layer and may or may not show systematic increase in [Sr] down one growth layer.

Equilibrium deposits should show consistent increase in [Mg] and [Sr] and constant [Mg]/[Sr] ratio in a growth layer.

*Stricter limits could be applied if precise values of λ^c_{Sr} and λ^c_{Mg} were available.

Detection of changes in water chemistry (between growth layers) poses the most difficult problem in interpretation of Mg and Sr distribution in equilibrium speleothem.

Isotopic equilibration and trace element equilibration are independent phenomena. Isotopic and trace element equilibria are established using different criteria.

For deposits formed in trace element and isotopic equilibrium, we expect to see a correlation between $\delta^{18}O$ and [Mg] in calcite speleothem.

CHAPTER III

RESULTS OF INVESTIGATION OF Mg AND Sr DISTRIBUTION IN SPELEOTHEM

Structure and Sampling of Speleothem

Most of the stalagmites studied were elongate consisting of growth layers which are thick at the apex and thin laterally. Variation in organic or trace element content, changes in crystal size or orientation, layers of fluid inclusions or detrital material may distinguish individual growth layers. Where changes in crystal size and orientation occur, it is usually due to the formation of many small crystals nucleating on detrital particles. In deposits which are free of detrital material crystals tend to be large cutting across and obscuring growth layers. A sharp change in orientation occurs between the apex and the flanks of elongate stalagmites so that the c axis retains an orientation perpendicular to the growth layer.

The thinning of growth layers away from the apex

creates a sampling problem. A sample of given size taken from the long axis of a stalagmite represents a far shorter period of time than a sample taken from the same layer away from the axis. The scale of flowstone deposits is much larger - individual 'delta lobes' of a flowstone may be several meters across. The thickness of individual layers decreases across the deposit at a far slower rate. Samples representing comparable periods of time may be taken at widely spaced points. This is important in establishing equilibrium deposition.

In many of the samples studied it was impossible to take comparable samples from individual growth layers. (A 0.1 g sample 3/16" in width represents at least 50 years of growth in an axial sample and 2-4 times that when taken on the edge of a stalagmite). In dealing with stalagmites two sets of samples were taken, one set located at intervals along the stalagmite axis (axial profile) and one set along a line oblique to this axis (oblique profile). The two sample sets cover the same period of deposition.

The second set consists of fewer samples each covering a wider time range - successive samples being located further from the axis and representing longer periods of time. The model for equilibrium deposition predicts that Mg and Sr concentrations will be higher in the second set of

samples and that Mg:Sr ratios in two sets will be similar. Peaks in Mg/Sr ratio caused by temperature would be expected to appear in both axial and oblique profiles.

Model for Equilibrium Mg:Sr Distribution in a Stalagmite

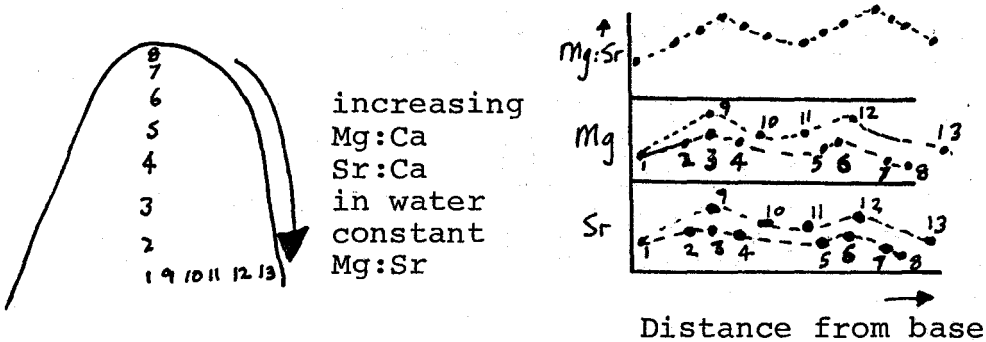

samples 1-8 constitute an axial profile; samples 1-13 constitute an oblique profile

(1st and 2nd sample sets interpolated using first and last points and any growth layers which can be traced)

Bulk solution of source rock has been assumed giving constant Mg:Sr ratio in the stalagmite to within 16 %. Variation in Mg:Sr ratio in seepage water or changing temperature would result in greater variation of Mg:Sr ratio between growth layers.

In a flowstone deposit (76008) four samples were taken from each of two growth layers. Samples from single growth layers were also taken from two stalagmites (76108 and 76190).

Sample #		Location	Mean Age Ka BP	$[\overline{Mg}]$ Axial Profile Only	$[\overline{Sr}]$	Mean Growth Rate cm/Ka BP	Remarks
76144	England	Ingleborough	?	935	35	?	Detrital contamination, accurate dating not possible. Low [Sr] precise determinations not made.
76190		Gavel Pot	9.9	362	152	8.2	Axial profile only
76130		Easegill Caverns	7.6	-	300	5.4	[Mg] increases away from stal axis. Need reanalysis of samples for reliable absolute values of [Mg]
76129		Easegill Caverns	5.1	1489	171	3.3	
76108	Yorkshire	White Scar	8.6	916	161	4.4	Axial and oblique profiles. 2 growth layers
76208		Gaping Gill	11.8	806	235	8.9	Axial and oblique profiles
76191		Gaping Gill	2.8	377	170	8.2	Clean core - axial profile obtained but impossible to trace growth layers into or obtain clean samples from flank
77143		Ingleborough	160	524	25	0.1	Oxygen and carbon isotope data available
75123		Cascade	53	1138	59	1.0	
76008		Cascade		777	38		Flowstone
GV2	West Va.	Grapevine Cave top 12 cm base 2 cm	78 160	1791 3171	86 123		Flowstone with oxygen and carbon isotope data

Summary of data on Sr and Mg distribution in speleothem

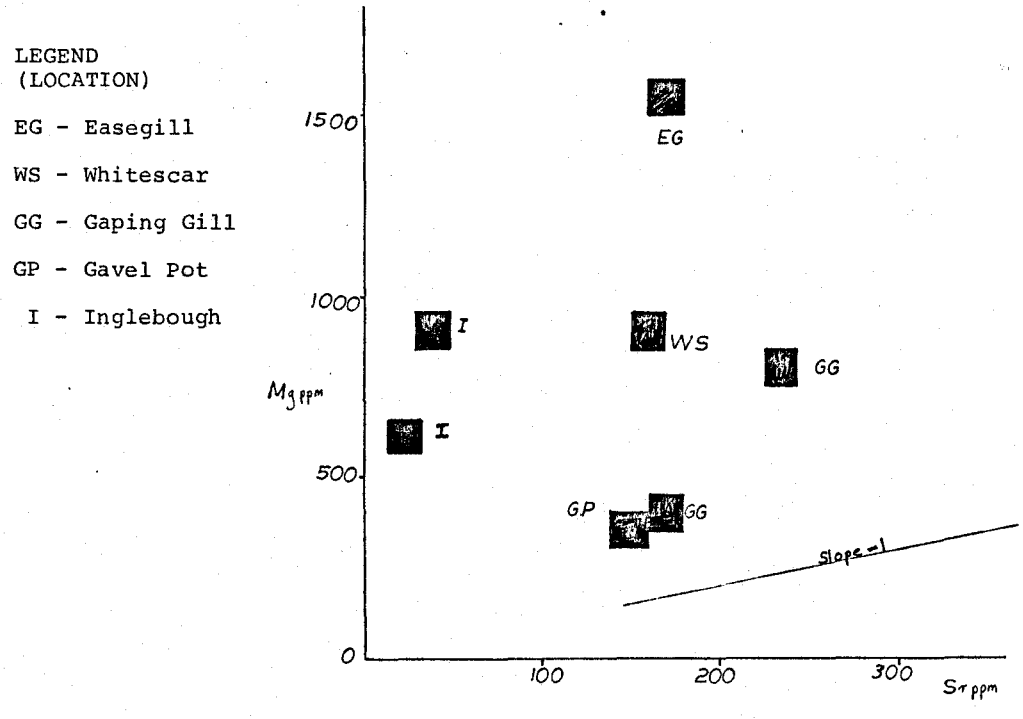

[Sr] and [Mg] mean values for English speleothem

Summary of Calculated Parameters for Speleothem

Summary of Calculated Parameters for Speleothem

Area	Sample	Calculated Minimum F_{Ca} Using Mg	Using Sr	Mg:Sr min.	max.	mean	% Variation from Mean
Yorkshire England	76129		0.7				?
	76108	0.5	0.4	2.8	12.9	6.4	101
	76144	0.6		13	38	27	?
	76190	0.5	0.5	1.5	4	2.7	44
	76191	0.7	0.7	1.7	2.8	2.2	27
	76208	0.7	0.5	2.5	5.5	4	37
	77143	0.6	0.4	12	40	23	74
	76130		0.5				?
West Virginia GV2	top 12 cm	0.6	0.5	16	28	21	33
	base 2 cm	0.85	0.9	27	24	24	13
Vancouver Island	75123	0.7	0.55	11	25	20	45
	76008	0.55	0.7	13	38	22	72

$$F_{Ca} \simeq \frac{[Sr]_i}{[Sr]_f} \simeq \frac{[Mg]_i}{[Mg]_f}$$

General Observations on Mg and Sr in Speleothem

For each deposit studied a minimum F_{Ca} was calculated using maximum and minimum Mg and Sr concentrations in all samples. These are estimates of the minimum proportion of calcite remaining in solution after precipitation of calcite between two sample points. In no case was calculated $F_{Ca} < 0.4$. Thus even allowing for large errors in estimating F_{Ca} we must explain variation of Mg:Sr ratio in excess of our previously calculated limit of 16% in terms of temperature variation in λ^{c}_{Mg} changing Mg:Sr ratio in solution or disequilibrium partitioning. If differing Mg and Sr concentrations in speleothem were due to different values of F_{Ca} in equilibrium deposits, we would expect to see points on a plot of Mg vs. Sr fall on a line of constant Mg:Sr ratio with a slope of 1. All deposits studied show variation in Mg:Sr ratio in excess of 16% (indicating disequilibrium partitioning or variation in temperature or TE:Ca initial ratios). Mean values of Mg and Sr for different deposits in the same area show no obvious relation to each other. Points within one speleothem fail to show a positive linear relation between Mg and Sr.

Distribution of Mg and Sr in individual speleothem must be considered in detail to determine whether equilibrium

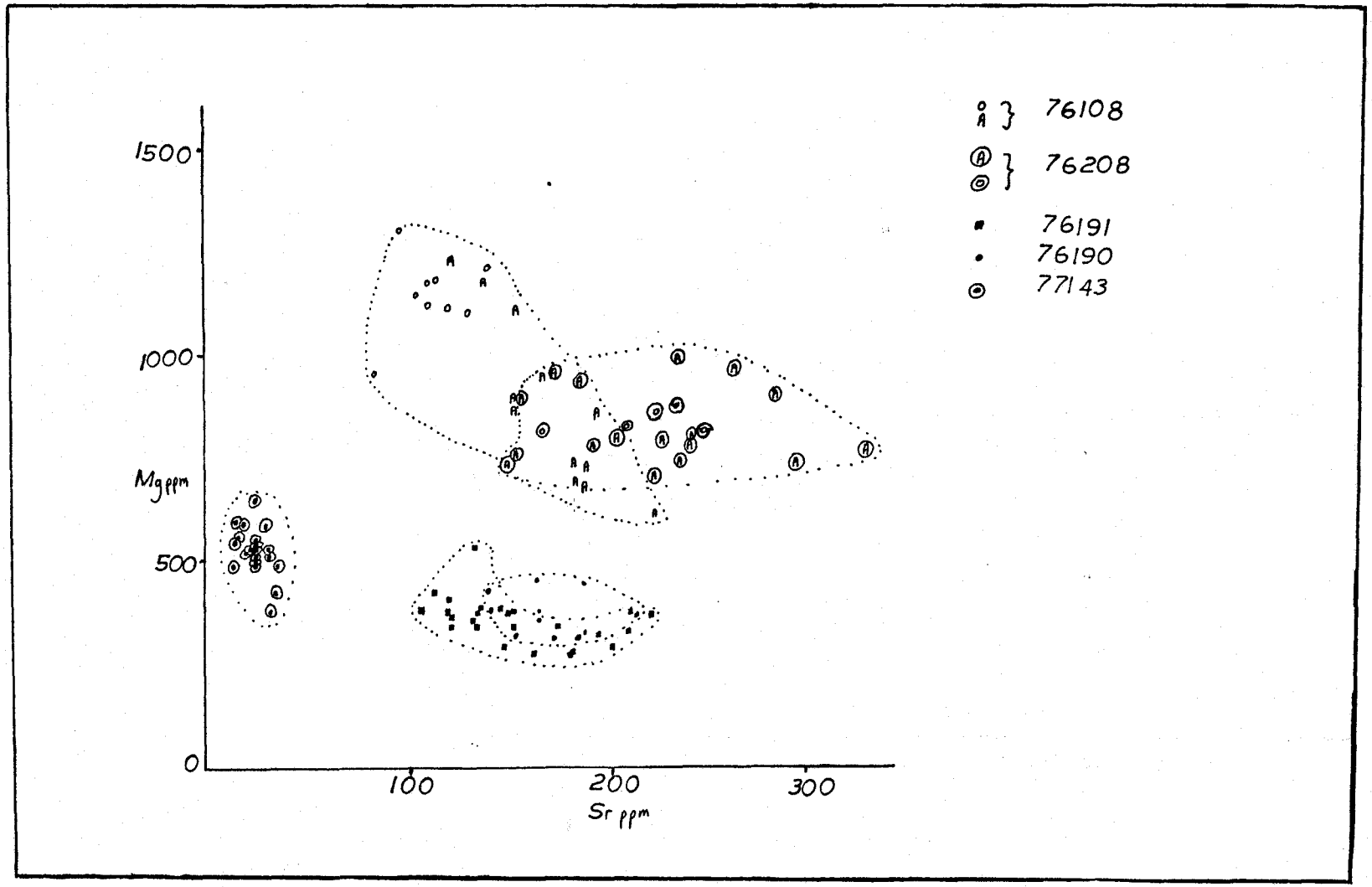

Sr correlation with Mg in speleothem - range of values for [Mg] and [Sr]

A = axial sample O = oblique sample

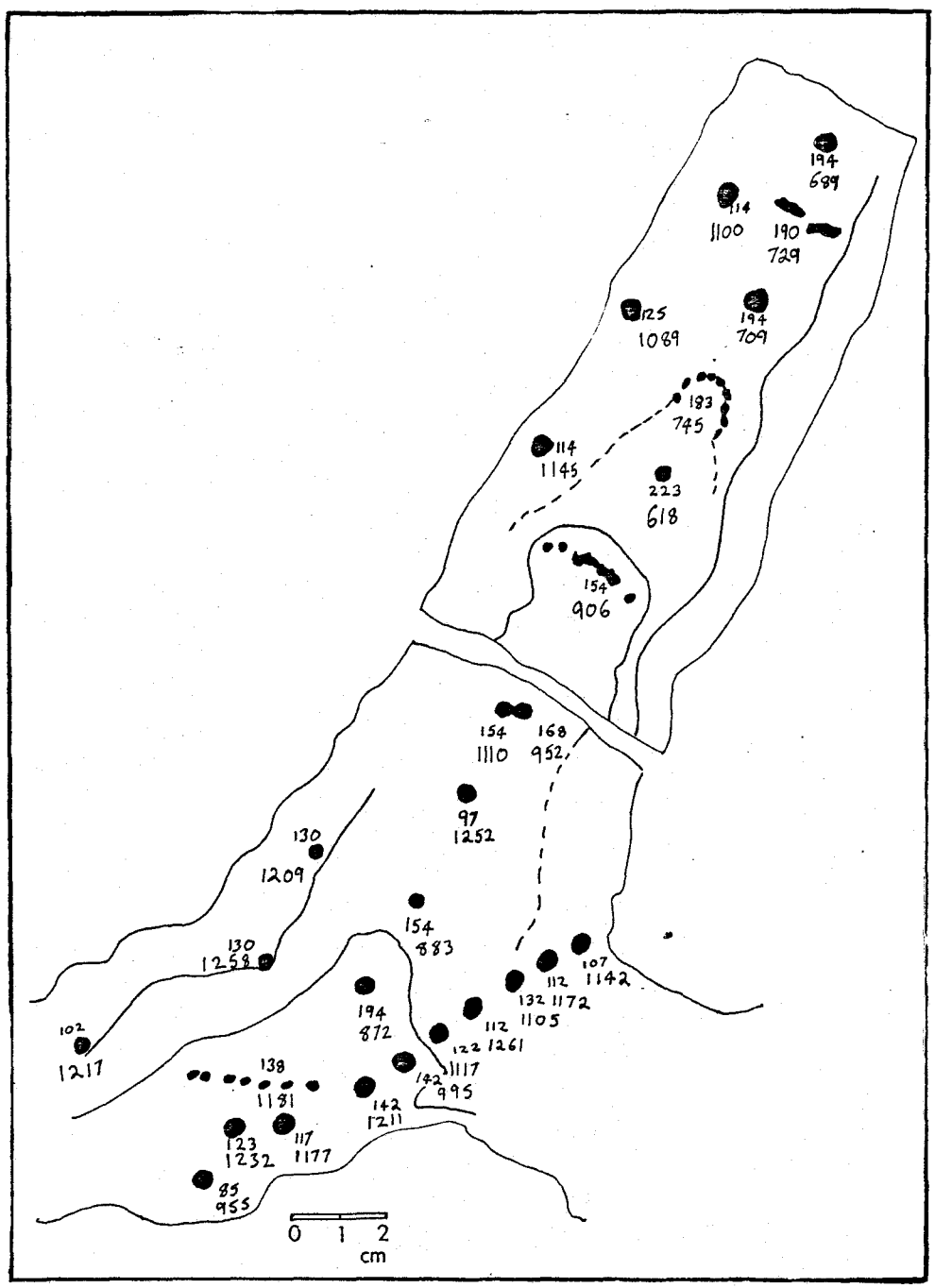

Distribution of trace elements in speleothem 76108
Top number Sr ppm; bottom number Mg ppm

deposition occurred. Large differences in Mg and Sr concentrations in different deposits probably reflect differences in source rock.

Discussion of Trace Elements in Individual Speleothem

English Speleothem

76108

As can be seen from the map of Sr concentration few growth lines were visible in this deposit. However, interpolation of the two profiles obtained assuming a constant proportionate difference between the thickness of calcite deposited along each profile, resulted in coincidence of peaks in Mg concentration. The Mg concentration for the two profiles varies in the manner predicted by the model for equilibrium deposition. The Mg:Sr ratio is variable (2.8-12.9). The Sr concentration decreases away from the

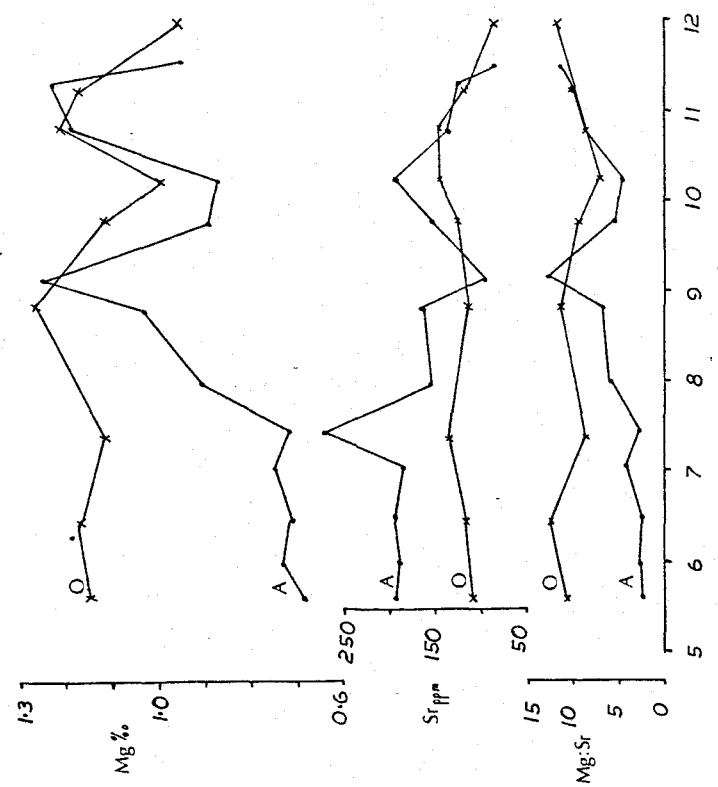

Distribution of Mg and Sr in speleothem 76108

stalagmite axis (in the oblique profile). Mg concentration, Sr concentration and Mg:Sr ratio are less variable in the oblique profile. This is probably the result of averaging over a longer time period, as previously discussed.

The decrease in Sr concentration away from the stalagmite axis is difficult to explain. Since Mg concentration behaves as predicted by the equilibrium model we do not seem to be looking at a sampling problem. A decrease in the apparent partition coefficient due to approach to equilibrium Ca concentration would explain a decrease in Sr concentration, provided the decrease in $\lambda_{Sr}^{c'}$ was enough to more than compensate for the increase in Sr:Ca ratio in solution.

Calculated minimum F_{Ca} for this deposit is 0.4. Thus a decrease of $\lambda_{Sr}^{c'}$ by a factor of 2 or more may be occurring. When a plot of Mg vs. Sr for this stalagmite is examined a negative correlation is obtained, even if only points on the axial profile are considered. Points in the oblique profile plot in the high Mg low Sr region of this field.

Change in $\lambda_{Sr}^{c'}$ is only one possible explanation. The presence of variable amounts of aragonite would also explain this. X-ray determinations should be made to check composition. No aragonite was detected by staining with Feigls solution. A vertical slice of the stalagmite was cut into

blocks. These blocks were polished and stained with Feigls solution as described by Katz et al. (1965). The blocks stained after about 25 minutes (as did scrapings from a calcite crystal used as a control). No earlier staining crystals were found. Feigls solution was also used to test an aragonite speleothem from Jamaica (J8); this gave a positive result staining in 5-10 minutes. Since this chemical test relies on the different solubilities of calcite and aragonite, results depend to a certain extent on surface area and number of crystal defects - they should be confirmed using other methods.

Thin sections were made from the blocks of the 76108 stalagmite. Large clean calcite crystals were seen. Finer crystals were seen at the base of some growth layers. These appeared to have nucleated on detrital particles and lacked the acicular form expected for aragonite. Sr and/or Mg adsorption on detritus and inclusion of detrital particles in the samples might have partly accounted for the inverse relation between Mg and Sr concentrations in this speleothem. However very little detrital material was seen in the sections examined. A very low Sr concentration was found in speleothem 76144 which contains considerable amounts of quartz and clay. No evidence for recrystallisation was seen in either deposit.

The following model is proposed to account for decreasing $[Sr]_s$ and increasing $[Mg]_s$ away from the stalagmite axis.

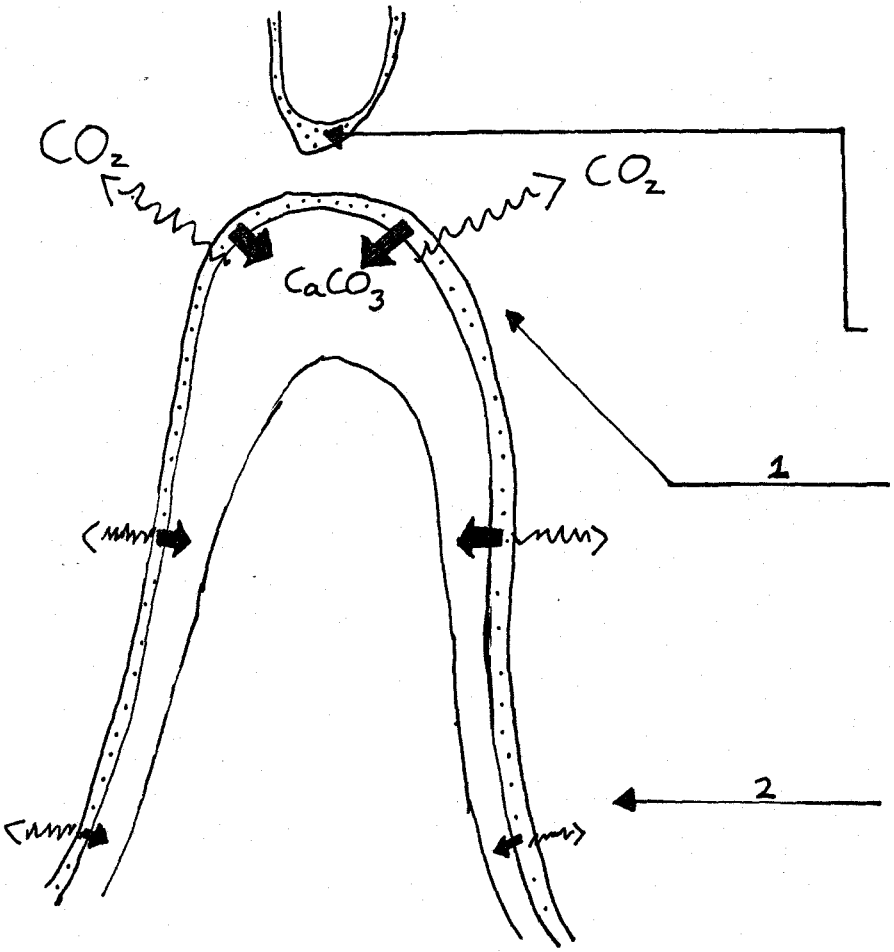

$$[Sr]_{L_1} \simeq [Sr]_{L_2}$$

$$[Mg]_{L_1} \simeq [Sr]_{L_2}$$

$$\lambda^{c'}_{Mg} = \lambda^{c'}_{Mg_2} \simeq \lambda^{c}_{Mg}$$

$$\lambda^{c'}_{Sr_1} > \lambda^{c'}_{Sr_2} > \lambda^{c}_{Sr}$$

Crystal size and orientation also change from the apex to the flanks of the speleothem.

Peaks in [Mg] occurring in both axial and oblique profiles might be due to kinetic effects, high temperature or high Mg:Ca ratio in seepage water.

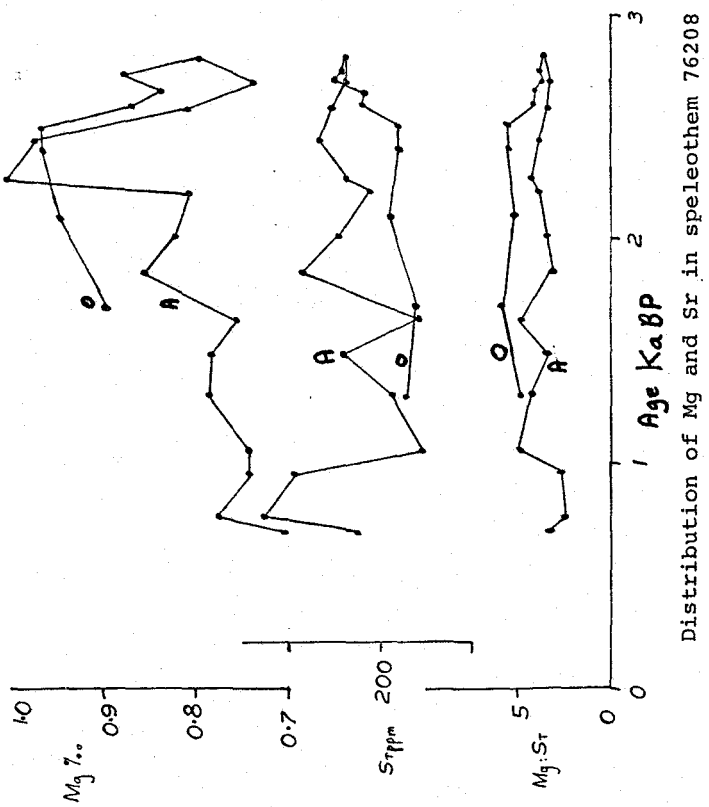

Distribution of Mg and Sr in speleothem 76208

76208

This stalagmite has a distribution of Mg and Sr similar to that found in 76108. The Mg:Sr ratio is considerably less variable. Plots of Mg vs. Sr show that the samples in the oblique profile fall toward the lower end of the range of Sr concentration, but have the same range of values for Mg concentration as samples in the axial profile. This would seem to indicate that smaller differences in proportion of calcite precipitated occur between samples in this deposit. Minimum calculated F_{Ca} is 0.5 (compared to 0.4 for 76108). Smaller changes in $\lambda^{c'}_{Sr}$ would result from smaller changes in saturation state.

The fields of Mg and Sr concentration for 76108 and 76208 overlap. This suggests similar sources of seepage water. These deposits were collected from different caves and are of different ages, but might have been fed by waters from the same geologic formation. A high initial P_{CO_2} would allow generation of supersaturated waters leading to extreme disequilibrium deposition. There is no way to determine whether these deposits have equilibrated with the Mg in solution.

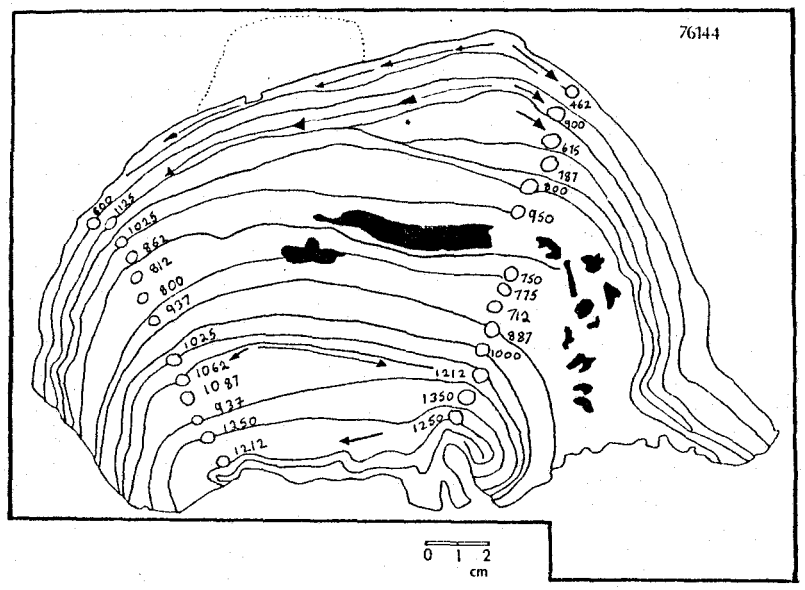

Numbers indicate [Mg] ppm in adjacent sample direction
← flow of drip water across speleothem

This speleothem owes its hemispherical shape to the approximately uniform thickness of many growth layers and to a constantly shifting axis (change in location of seepage water drip). Ironically layers of detrital material which make for easily mapped growth layers make accurate dating impossible. Detrital material was probably introduced by periodic flooding of the cave.

76144

If supersaturation and rapid precipitation of calcite cause the characteristic elongate stalagmite shape, then deposits formed under conditions of uniform infinitesimal supersaturation will tend to have layers which vary far less in thickness. Such deposits should be characterised by a relatively less elongate shape, relatively low [Sr] and constant Mg:Sr ratio. The speleothem 76144 has a uniformly low [Sr] (of about 35 ppm). It is roughly hemispherical. Sample size did not allow precise determination of Sr in this stalagmite.

The map opposite shows that the growth layers are approximately uniform in thickness. However, this is probably due to nucleation of many small crystals on the layers of detrital material defining growth layers (see photographs of thin sections). No conclusions may be made about equilibrium vs. disequilibrium for this deposit.

77143

This deposit has similar Mg and Sr concentration to 77144; it was collected in the same cave. These deposits may have been fed by waters from the same source rock.

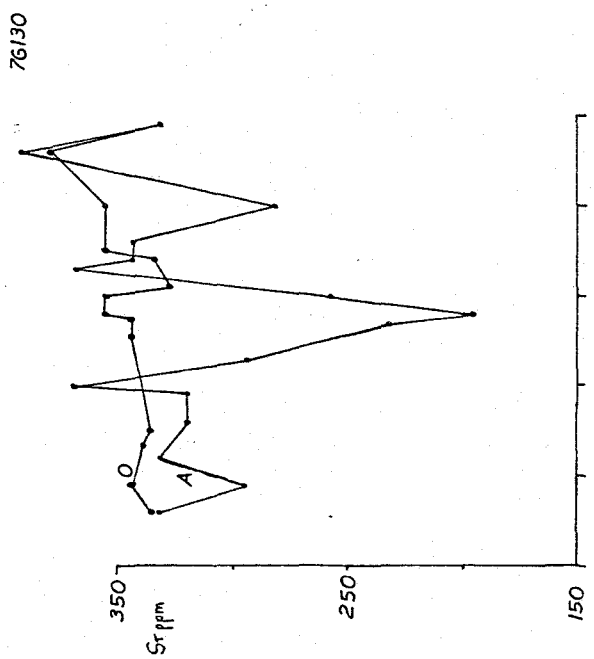

Distribution of Sr in speleothem 76130

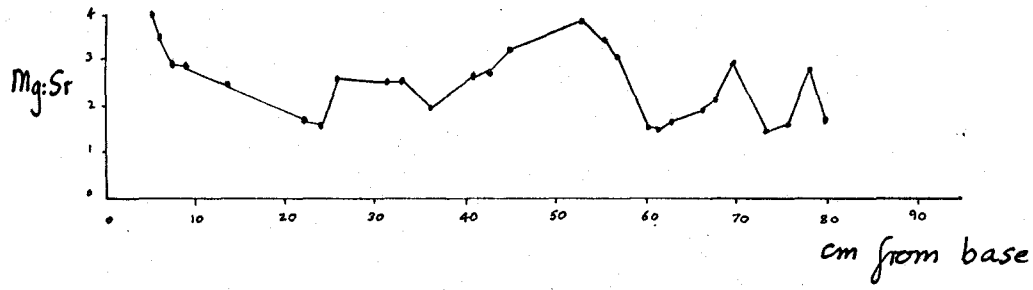

Variation in Mg:Sr ratio - axial profile speleothem 76190

76130

Sr concentrations in axial and oblique profiles in this deposit are comparable. There appears to be an increase in Sr concentration away from the stalagmite axis. This could be an equilibrium deposit. Approximate values for Mg concentrations were obtained, Mg:Sr ratio appears to have varied only slightly. However, precise values of Mg concentrations have not been obtained due to technical problems.

76191-76190

The fields of Mg and Sr concentrations for these deposits overlap, similar source waters are indicated. Mean values of Mg:Sr ratio are very similar (2.2 and 2.7). Variation in axial Mg:Sr ratio is >100% in each case (but far less than for 76108). Sr concentrations are similar to those in 76108 and 76208, but Mg concentration is considerably lower.

An attempt was made to obtain samples from one growth layer in 76190 (a small 3/32" drill bit was used). Maximum separation of samples laterally was about 15 cm. Very little variation in Mg or Sr concentrations was seen in this distance. Mg:Sr ratio in 76190 shows a smooth variation through time.

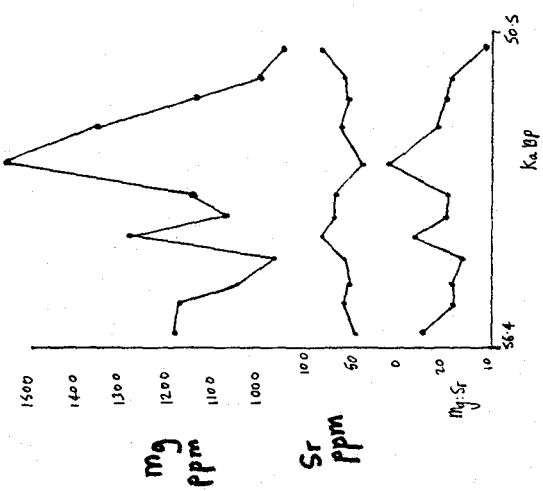

Axial trace element profile - speleothem 75123

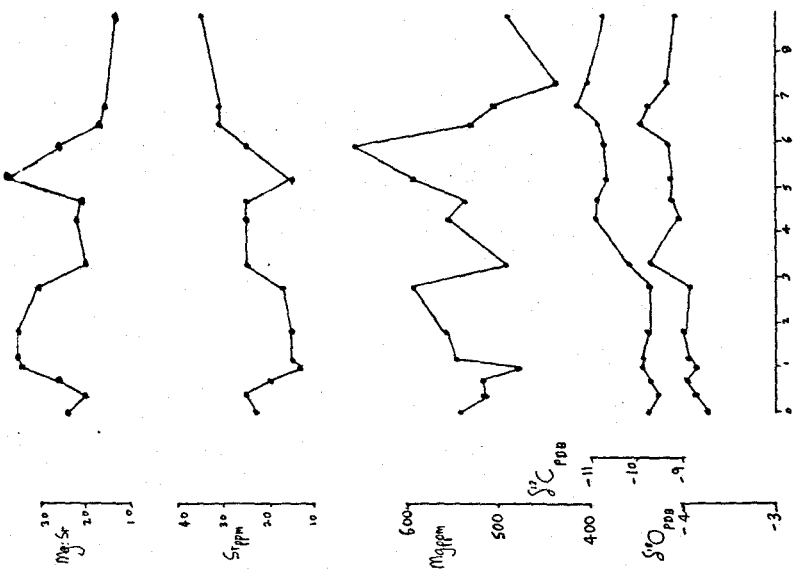

Distribution of Mg and Sr, comparison with isotopic composition, speleothem 77143

Vancouver Island Speleothem

76008

Analyses for Mg at four different points in each of two growth layers in 76008 showed no significant variation. This means that no significant change in F_{Ca} occurred over this short distance (about 7 cm). Mg:Sr ratios for this deposit are high because of low Sr concentrations (Mg:Sr ratio varies from ∿16 to ∿38).

75123

In speleothem 75123 erratic changes in Mg and Sr concentration occur causing extremely variable Mg:Sr ratios. Sr concentrations are similar to those in 76008.

General Conclusions Based on Mg and Sr Distribution in Speleothem

Smooth variation in Mg, Sr and Mg:Sr ratio may occur in speleothem. Fluctuation about a mean value rather than definite trends or abrupt changes suggests that Mg:Sr ratio in the seepage water has not changed significantly through time for these deposits. Similar values of Mg:Sr ratios in speleothem suggest similar Mg:Sr ratios in seepage water.

Bearing in mind the high values of $\lambda_{Sr}^{c'}$ measured by

Holland et al. in the cave environment, it is not unreasonable to attribute much of the fluctuation in Mg:Sr ratios in speleothem to variation in $\lambda^{c'}_{Sr}$. The observation that [Mg] has always been found to increase rather than decrease away from the stalagmite axis is strong evidence that $\lambda^{c'}_{Mg}$ is less sensitive to saturation state than $\lambda^{c'}_{Sr}$.

Mg and Sr concentrations could be used to find Mg:Ca and Sr:Ca ratios in evolving cave waters. Only equilibrium deposits may be used for this purpose. Mg concentrations of >1000 ppm are found in the speleothem studied, a $[Mg/Ca]_s$ value of 10^{-3} in calcite speleothem indicates $[Mg/Ca]_L$ of 10^{-1}-10^{-2} in seepage waters (depending on which values are adopted for λ^{c}_{Mg}). Sr concentrations in speleothem indicate low Sr:Ca ratio in seepage waters in all cases. Estimates of Sr:Ca ratio in solution based on λ^{c}_{Sr} will be overestimates since $\lambda^{c'}_{Sr} > \lambda^{c}_{Sr}$. 300 ppm Sr in speleothem indicates Sr:Ca ratios in parent waters of $3.75.10^{-4}$-5.10^{-4} depending on which values of λ^{c}_{Sr} are adopted. The deposits studied were from limestone areas. Sr:Ca ratios in waters from limestone areas do not usually differ from that in the source rock (Skougstad and Horr, 1963). An average Sr:Ca ratio for limestone of 6.1×10^{-4} was quoted by them. Our estimated estimated Sr:Ca ratios for seepage waters are of the same order of magnitude.

Using Gascoyne's values of λ^{c}_{Mg}, 0.02 at 7°C and 0.04 at ∿23°C, we get changes in $[Mg]_s$ of 100% in ∿15°C. Fluctuations of 100% occur over a fairly short time span in these deposits (<5 Ka). If we are to interpret $[Mg]_s$ in terms of temperature we require some means of determining F_{Ca}. Secular changes in [Mg] in different deposits in the same area should change in the same way in response to climate. Unfortunately complete Mg data for the English speleothem is not yet available.

Comparison of Trace Element Composition with Isotopic Composition

Mg and Sr determinations were carried out for samples from two deposits which had been demonstrated to be in isotopic equilibrium. Only one set of samples has been analysed from each. Equilibrium trace element partitioning has not been demonstrated.

77143

Large fluctuations in Mg:Sr ratio may be due to disequilibrium deposition, variable Mg:Sr ratios in seepage waters or temperature changes. There appears to be an

inverse correlation between Mg and Sr in that peaks in Sr concentration correspond to troughs in Mg concentration. No statistically significant correlation exists. If there is a tendency for low Sr to accompany high Mg the relationship is not a simple linear one.

No significant correlation between isotopic and trace element composition was found. An attempt to compare waters which had precipitated similar proportions of calcite was made. Assuming constant initial Mg:Ca ratio, $[Mg]_s \alpha F_{Ca}$*. By comparing calcite of different [Mg] we should be able to detect effects which would otherwise be masked by variable degree of evolution of the water. Using [Mg] as the abscissa we see a parallel variation in [Sr] and isotopic composition.

---

*Temperature effects would be masked by significant change in Mg:Ca in solution.

The erratic nature of the 'trends' obtained in this way may be explained if we remember that only adjacent points are directly comparable. Although increasing [Mg] implies increasing F_{Ca} we also have to consider the effects of temperature, initial composition and rate of precipitation on the remaining variables.

$$[Sr]_s = f \begin{pmatrix} \text{(composition of water} \\ \text{(rate of precipitation)} \\ \text{(temperature?} \end{pmatrix}$$

$$\delta^{13}C = f \begin{pmatrix} \text{(composition of water} \\ \text{(rate of precipitation)} \\ \text{(temperature} \end{pmatrix}$$

$$\delta^{18}O = f \begin{pmatrix} \text{(composition of water} \\ \text{(rate of precipitation)} \\ \text{(temperature} \end{pmatrix}$$

Temperature is a variable in each case since complete T-independence for λ^{c}_{Sr} at low temperatures has not been proven and since approach to equilibrium may in itself be T-dependent.

The existence of a parallel variation in these quantities using Mg (αF_{Ca}) as an abscissa could be spurious. More data is needed to establish a true correlation. Perhaps the most logical approach to the problem of statistical analysis in this case would be to subdivide the data points using Mg concentration. Points of similar Mg concentration should

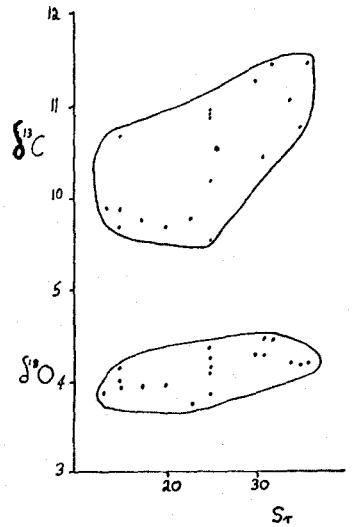

Comparison of isotopic composition and Sr concentration in speleothem 77143

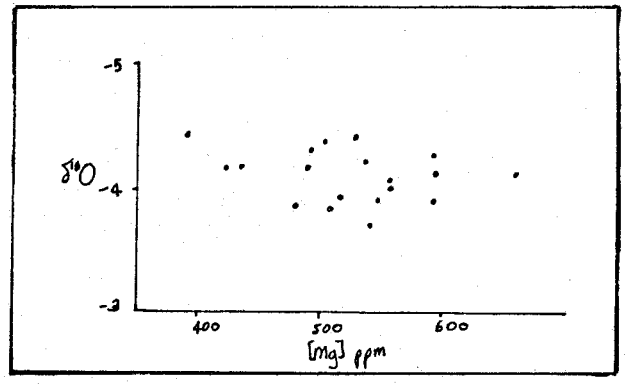

Comparison of isotopic composition and Mg concentration in speleothem 77143

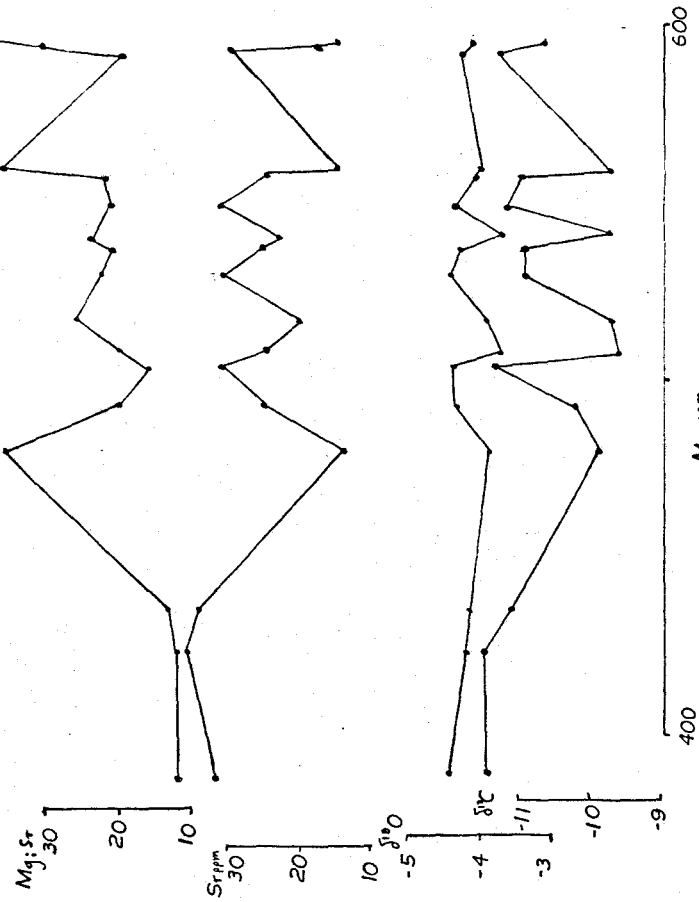

Mg vs. Sr, $\delta^{18}O$ and $\delta^{13}C$ in speleothem 77143

show a correlation between Sr concentration and isotopic composition if the apparent parallel variation is a real one. Variation in Mg and Sr concentrations and Mg:Sr ratio in single growth layers in this deposit should be examined. No parallelism between isotopic composition and Mg concentration is observed using [Sr] as the abscissa.

The Grape Vine Speleothem

Isotopic compositions were interpolated from Thompson's earlier work on other parts of this deposit.

No significant correlation between Mg and Sr is found, peaks in Mg and Sr concentration do coincide. A drop in Mg and Sr concentration occurs after a break in deposition (at about 2 cm above the base). Mg:Sr ratio is variable (16-28). This could well be due to change in Mg:Sr ratio in seepage waters. No correlation between isotopic composition and trace element composition could be found using Mg concentration or distance from base as the abscissa to display data. Using [Sr] as the abscissa we find that $\delta^{18}O$ and Mg concentrations show a parallel variation. This could be explained by assuming equilibrium deposition, and constant initial Sr:Ca ratio. Changes in [Mg] for points of equal or similar [Sr] would reflect changes in initial Mg:Ca ratio and/or λ^{c}_{Mg}. Changes in $\delta^{18}O$ may also reflect changes in water

composition and/or changes in the isotopic fractionation factor. We could attribute parallel changes in [Mg] and $\delta^{18}O$ to climatic effects. Again more data is required to establish a real parallel variation.

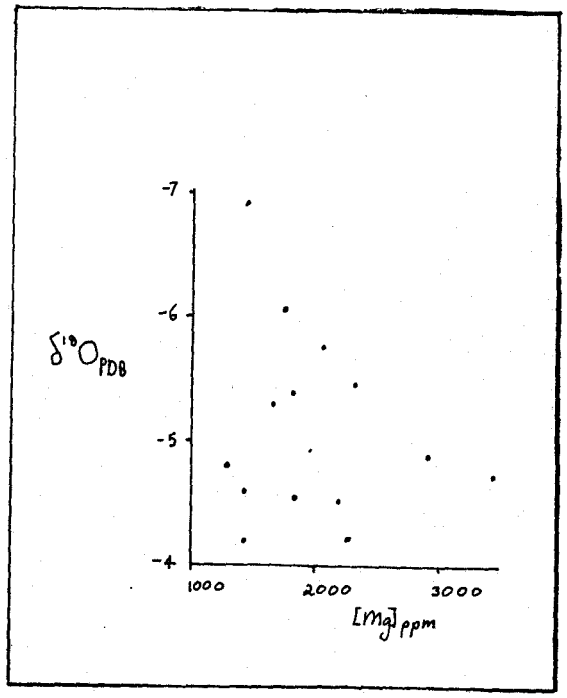

Mg vs. $\delta^{18}O$ for the Grape Vine Speleothem GV2

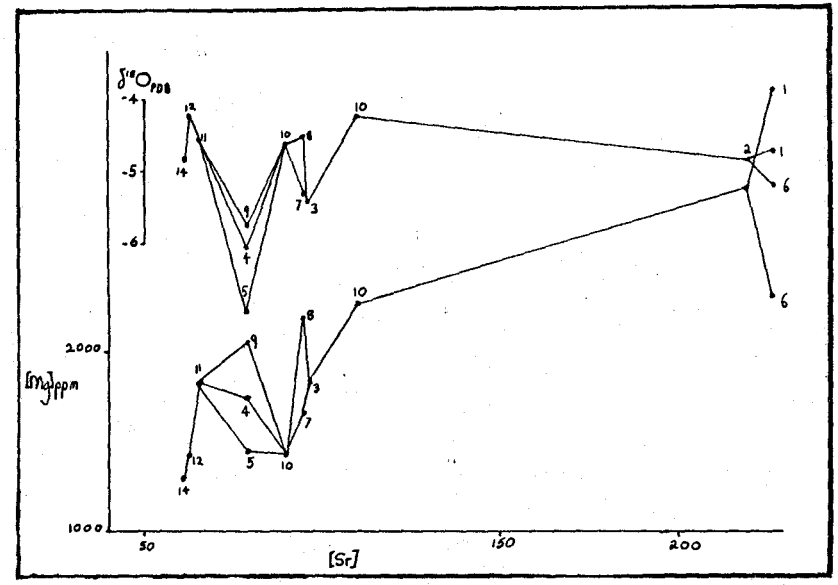

Mg vs. $\delta^{18}O$ for GV2 using [Sr] as the abscissa

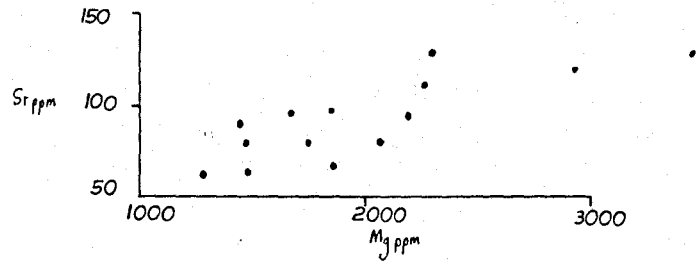

Mg vs. Sr in Grape Vine speleothem GV2

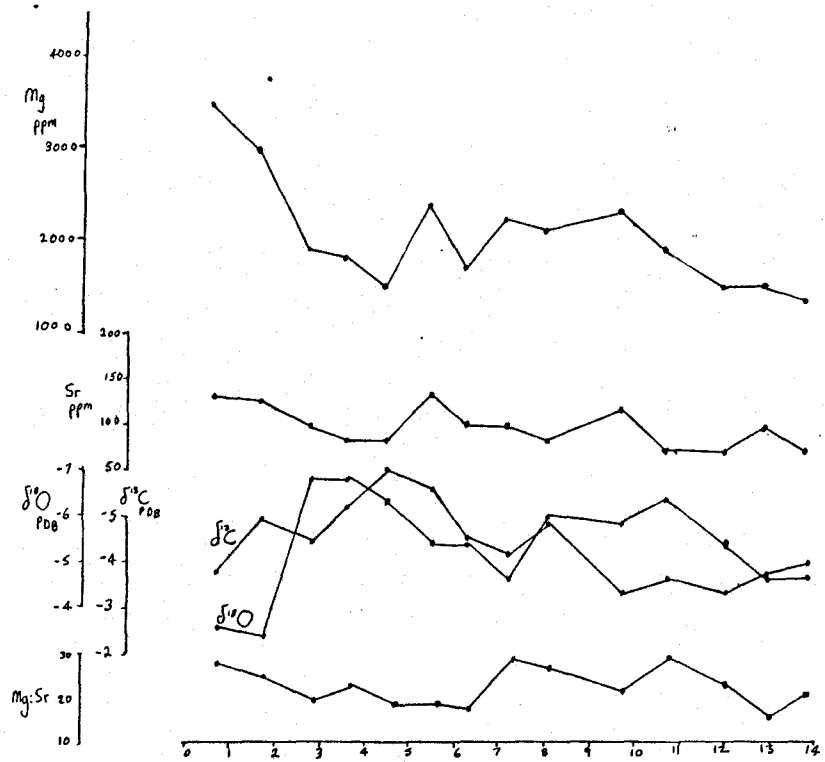

Distribution of Mg and Sr in the GV2 speleothem - Grape Vine Cave, West Virginia. Comparison with isotopic compositional variation.

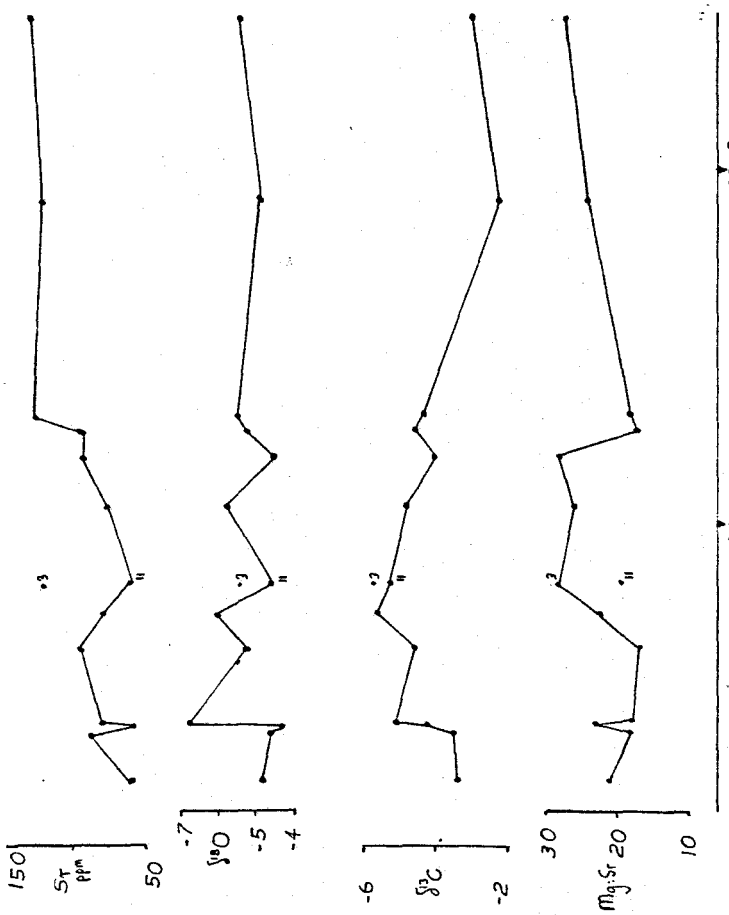

Mg vs. Sr in $\delta^{18}O$ and $\delta^{13}C$ in the Grape Vine speleothem GV2

PETROGRAPHY - LOCATION ORIENTATION AND PHOTOGRAPHS OF THIN SECTIONS

76108

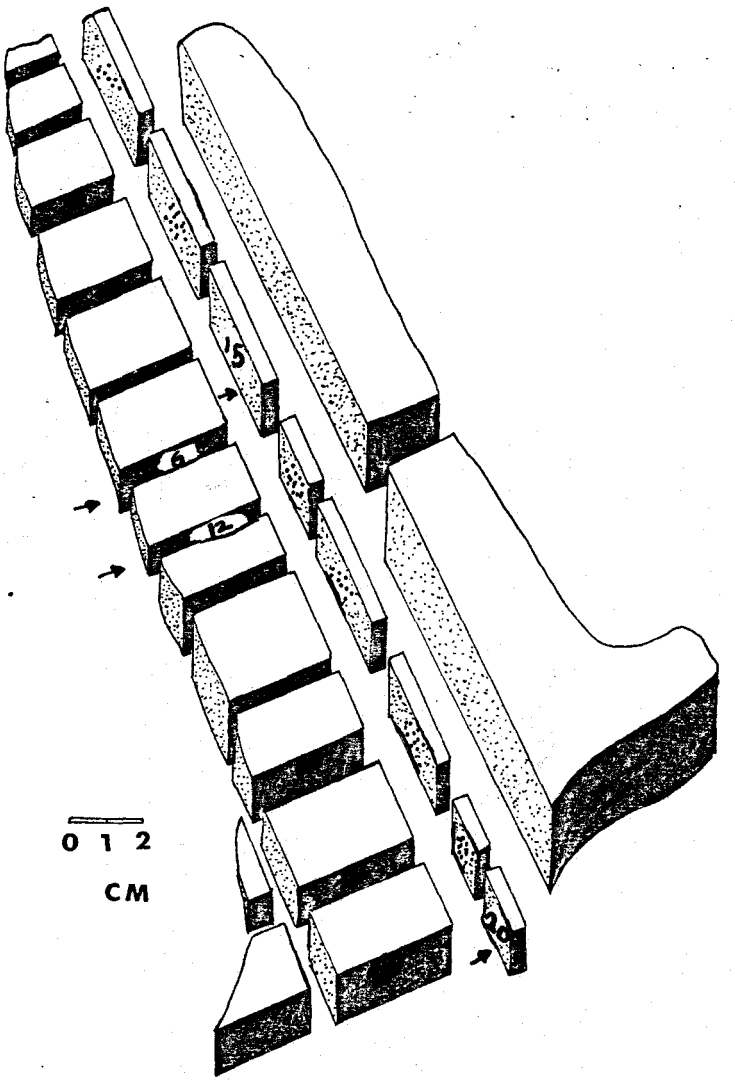

→ Locations of thin sections - speleothem 76108

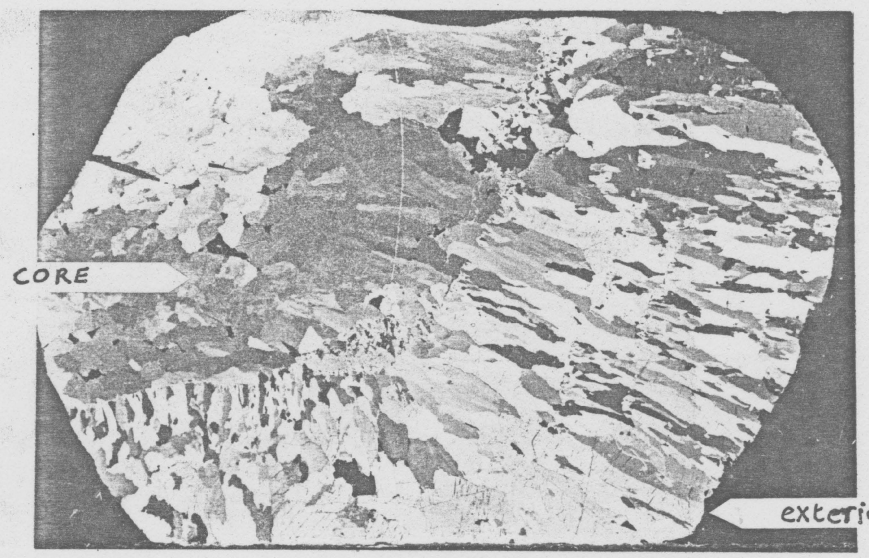

6

×4

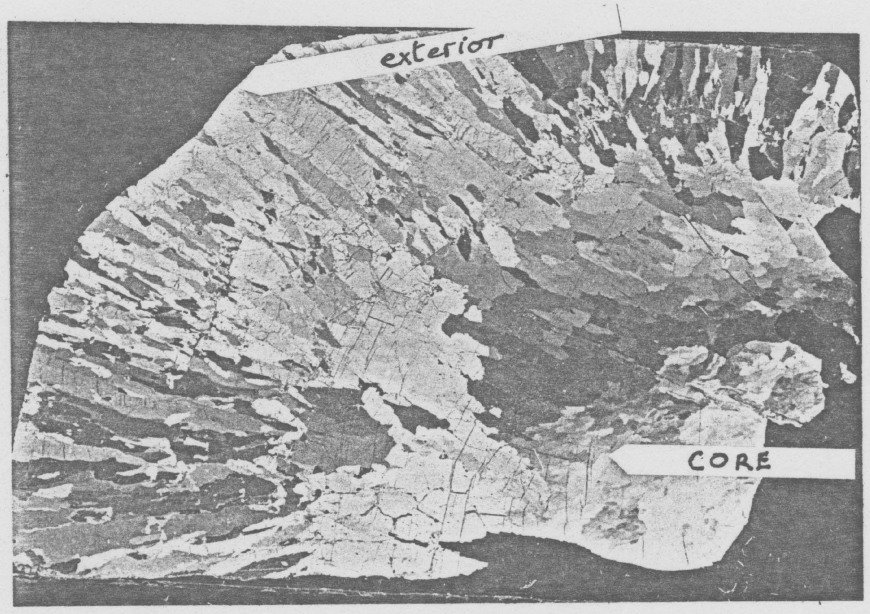

12

×4

Plate I. 76108-6 and 12. Note the change in crystal size and orientation from the core of the speleothem to the exterior.

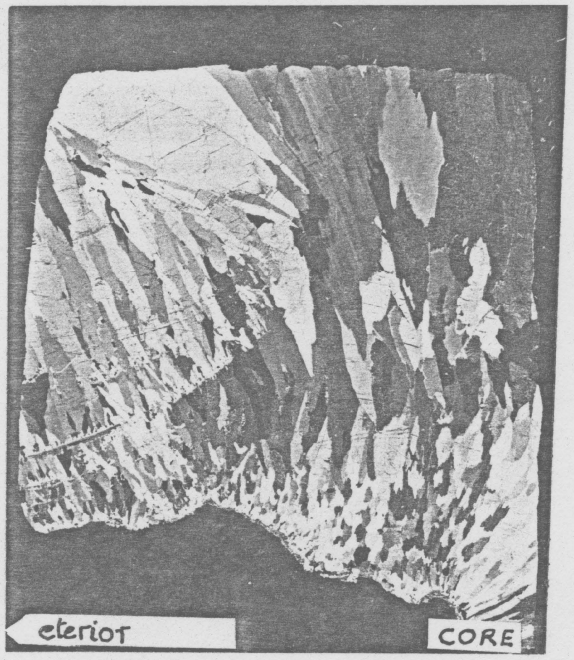

Plate II. 76108-20 - base of stalagmite. Note the sequence from fine to coarse crystals from detrital layers upward. Nucleation of many small crystals occurs on detrital particles.

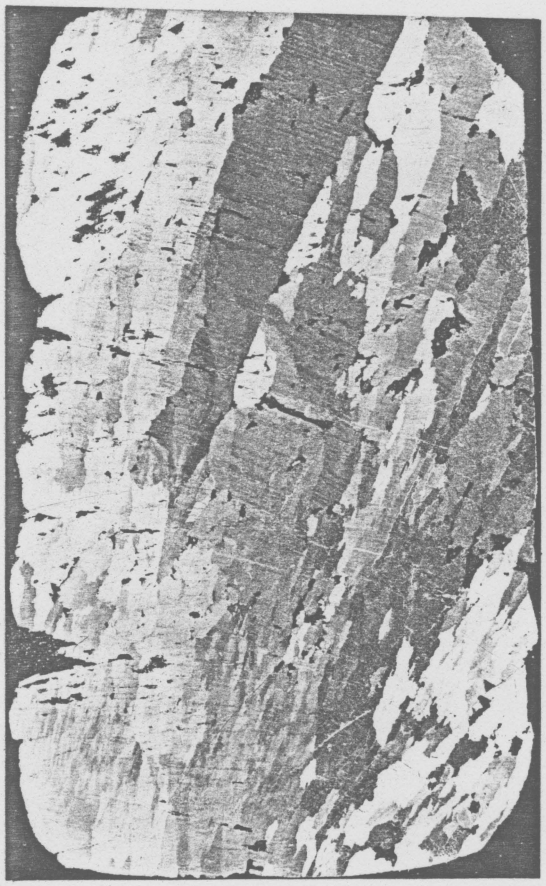

Plate III. 76108-15. Layers of fluid inclusions are visible.

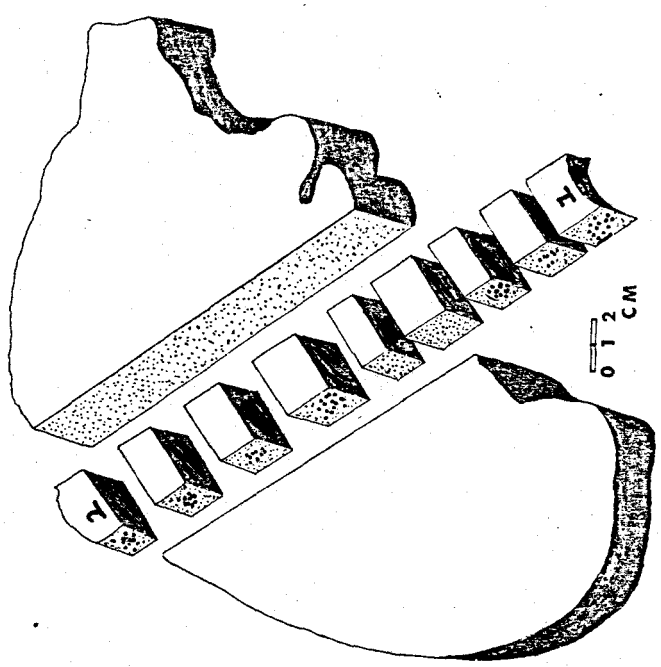

Locations of thin sections - speleothem 76144

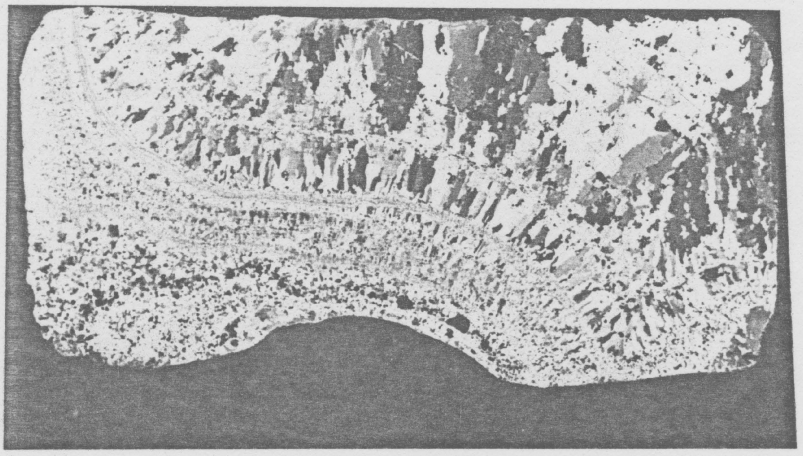

1

axis

×4

BASE

TOP

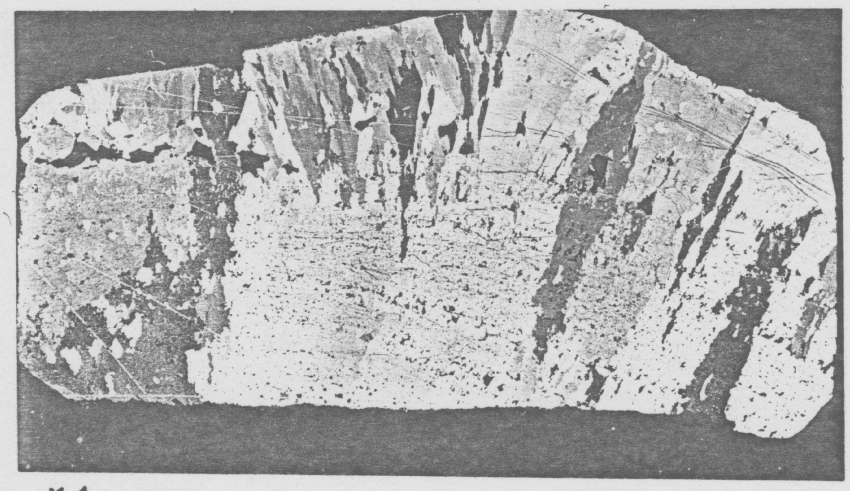

2

axis

×4

Plate IV. 76144. The crystal size is reduced - nucleation of many small crystals on detrital layers occurs repeatedly.

CHAPTER IV

DISCUSSION AND CONCLUSIONS

Mg:Ca and Sr:Ca ratios in cave seepage waters depositing speleothem increase as $CaCO_3$ is precipitated. This fact could be used to determine orientation of speleothem samples with respect to the seepage water input. Neither [Mg] nor [Sr] may be used in isolation as indicators of initial seepage water composition. However Mg:Sr ratio in deposits formed in equilibrium with Mg and Sr in seepage water should be a measure of the Mg:Sr ratio in that water.

Constancy of Mg:Sr ratio in a growth layer indicates precipitation in equilibrium with these trace elements in seepage waters. $\lambda^{c'}_{Sr}$ appears to be more rate sensitive than $\lambda^{c'}_{Mg}$.

Mg concentration in speleothem can be used to estimate the proportion of calcite precipitated. This requires the assumption that $\lambda^{c'}_{Mg}$ is approximately constant and equal to λ^{c}_{Mg}, and that changes in Mg:Ca ratio in the water mask changes in λ^{c}_{Mg} due to temperature. Parallel variation in

in [Sr], $\delta^{18}O$ and $\delta^{13}C$ was found for one deposit formed in isotopic equilibrium when these variables were plotted using [Mg] as the abscissa. More data is required to establish this parallelism. A parallel variation using Mg as abscissa might be due to comparison of waters which have precipitated a similar proportion of their dissolved $CaCO_3$, removing 'noise' caused by varying amounts of evolution. Other factors must then be invoked to explain why Sr, $\delta^{18}O$ and $\delta^{13}C$ behave in the same manner. A few of the variables involved have been discussed.

Assuming Sr:Ca initial ratios are constant and $\lambda_{Sr}^{c'} = \lambda_{Sr}^{c}$, $[Sr]_s$ may be used to estimate F_{Ca}. Parallel variation in $\delta^{18}O$ and [Mg] was found in one speleothem (GV2) using [Sr] as the abscissa. This could be interpreted in terms of climatic variation.

Further investigation of these and other deposits formed in isotopic equilibrium would establish whether the observed parallel variations in isotopic and trace element composition are significant. Investigation of Mg and Sr in single growth layers is needed. Widely spaced samples should be obtained since significant variation in $[Mg]_s$ or $[Sr]_s$ will occur only when significant change in $[Ca]_L$ has occurred.

A progression from disequilibrium toward equilibrium

occurs as supersaturated seepage waters approach equilibrium $[Ca]_L$. The characteristic elongate shape of many speleothem may be due to initially rapid precipitation of $CaCO_3$ from a supersaturated solution followed by a slower precipitation as the water approaches equilibrium. (Supersaturation of seepage waters with $CaCO_3$ has been observed in the cave environment; Holland, 1964; Thrailkill, 1971).

So far partitioning of Sr has been considered independent of crystal size. A drop in [Sr] in 76108 and 76208 occurs going from the coarse crystals forming the stalagmite axis to the finer crystals forming the flanks. A dependence on crystal size or morphology would certainly explain the lack of interlaboratory agreement on determination of λ^c_{Sr}. Perhaps this point should be investigated further.

Temperature dependence of $[Mg]_s$ in speleothem may only be detected if we can estimate the seepage water Mg:Ca ratio. We also need reliable determinations of λ^c_{Mg}. More data is needed before $[Mg]_s$ in speleothem may be interpreted in terms of temperature.

REFERENCES

FOLK, R.L. and ASSERETO, R., 1976. Comparative fabrics of length slow and length fast calcite and calcitized aragonite speleothem Carlsbad caverns, New Mexico. Jour. Sed. Petrol., 46, 3, 486-496.

GASCOYNE, M., 1979. Ph.D., in preparation.

GASCOYNE, M., SCHWARCZ, H.P. and FORD, D.C., 1978. Uranium series dating and stable isotope studies of speleothems. I. Theory and techniques. B.C.R.A., 5, 2, 91-111.

GLOVER, R.R., 1977. Caves and karst of the Yorkshire Dales. Int. Cong. Speleol. Guidebook, B.C.R.A.

HENDY, C.H., 1971. The isotopic geochemistry of speleothems. I. The calculation of the effects of different modes of formation on the isotopic composition of speleothems and their applicability as paleoclimate indicators. Geochim. Cosmochim. Acta, 35, 801-824.

HOLLAND, H.D., BORCSIK, M., MUNOZ, J. and OXBURGH,V.M., 1963. The coprecipitation of Sr^{2+} with aragonite and of Ca^{2+} with strontianite between 90 and 100°C. Geochim. Cosmochim. Acta, 27, 957-977.

HOLLAND, H.D., HOLLAND, H.J. and MUNOZ, J.L., 1964a. The coprecipitation of cations with $CaCO_3$. II. The coprecipitation of Sr^{2+} with calcite between 90 and 100°C. Geochim. Cosmochim. Acta, 28, 1287-1302.

HOLLAND, H.D., KIRSIPU, T.V., HUEBNER, J.S. and OXBURGH, V.M., 1964b. On some aspects of the chemical evolution of cave waters. Jour. Geol., 72, 36-67.

JOSHI, M.S., 1960. Precipitation of carbonates from sea water. Prog. Rep., U.S. A.E.C. Contract No. AT (30-1)-2266.

KATZ, A., 1973. The interaction of magnesium with calcite during crystal growth at 25-90°C and 1 atmosphere. Geochim. Cosmochim. Acta, 37, 1563-1586.

KATZ, A. and FRIEDMAN, G.M., 1965. The preparation of stained acetate peels for the study of carbonate rocks. Jour. Sed. Petrol., 35, 248-249.

KATZ, A., SASS, E., STARINSKY, A. and HOLLAND, H.D., 1972. Sr behaviour in the aragonite-calcite transformation: an experimental study at 40-98°C. Geochim. Cosmochim. Acta, 36, 481-496.

KENDALL, A.C. and BROUGHTON, P.L., 1977. Discussion - calcite and aragonite fabrics, Carlsbad Caverns. Jour. Sed. Petrol., 46, 486-496.

KENDALL, A.C. and BROUGHTON, P.L., 1978. Origin of fabrics in speleothems composed of columnar calcite crystals. Jour. Sed. Petrol., 48, 2, 519-538.

KINSMAN, D.J.J., 1969. Interpretation of Sr^{2+} concentrations in carbonate minerals and rocks. Jour. Sed. Petrol., 39, 486-508.

KINSMAN, D.J.J. and HOLLAND, H.D., 1969. The coprecipitation of cations with $CaCO_3$. IV. The coprecipitation of Sr^{2+} with aragonite between 16° and 96°C. Geochim. Cosmochim. Acta, 33, 1-18.

KITANO, Y., 1962. The behaviour of various inorganic ions in the separation of $CaCO_3$ from a bicarbonate solution. Bull. Chem. Soc. Japan, 35, 1973-1980.

KITANO, Y., KANAMORI, N. and OOMORI, T., 1971. Measurements of distribution coefficients of Sr and Ba between carbonate precipitate and solution. Abnormally high values of distribution coefficients measured at early stages of carbonate formation. Geochem. Jour., 4, 187-206.

LANGMUIR, D., 1971. The geochemistry of some carbonate groundwaters in central Pennsylvania. Geochim. Cosmochim. Acta, 35, 1023-1045.

McINTIRE, W.L., 1963. Trace element partition coefficients - a review of theory and applications to geology. Geochim. Cosmochim. Acta, 27, 1209-1264.

MOORE, G.W., 1956. Aragonite speleothems as indicators of paleotemperature. Amer. J. Sci., 254, 746-753.

MURRAY, J.W., 1954. The deposition of calcite and aragonite in caves. Jour. Geol., 62, 481-492.

SCHWARCZ, H.P., 1979. Pers. comm.

SKOUGSTAD, M.W. and HORR, C.A., 1963. Occurrence and distribution of Sr in natural waters. U.S. Geol. Surv. Water Supply Paper 1496-D, 97pp.

THRAILKILL, J., 1971. Carbonate deposition in Carlsbad Caverns. Jour. Geol., 79, 683-695.

APPENDIX I

PREPARATION OF STALAGMITE SAMPLES FOR TRACE ELEMENT ANALYSIS

Samples were taken along two lines from base to surface on a longitudinal section of each stalagmite. Before removing samples the surface was etched with 1M HCl and rinsed with distilled deionised water (DDH_2O). This provided a clean surface and accentuated growth layers. After sampling the cut surface was photocopied to record the position of sample holes.

Samples were removed using a hand held electric drill with a 3/16" drill bit. The following procedure was used:

(1) Roughly 0.1 g of powder was drilled and tipped onto a clean weighing paper.

(2) 0.1 g of powder was accurately weighed into a small glass vial. Samples were weighed to within 0.0002 g of 0.1 g. Samples which were to be dissolved immediately were weighed into a beaker.

(3) Samples were dissolved in a beaker covered with a watch glass to prevent loss of sample by effervescence. 1 ml 3 M HCl was added using a pasteur pipette. The sample was allowed to dissolve completely.

(4) The solution was poured into a 25 ml volumetric flask. DDH_2O was used to rinse beaker and watch glass; washings were added to the flask. The sample was made up to 25 ml with DDH_2O. The flask was stoppered and inverted several times to obtain a homogeneous solution.

(5) The sample was stored in a previously labelled polyethylene bottle.

(6) A clean dry pipette was used to transfer 5 ml of the sample to a clean 25 ml volumetric flask. This was made up to 25 ml with DDH_2O, homogenised and stored as before.

The above procedure yielded samples at 1600 and 320 ppm Ca (assuming $\sim$100% $CaCO_3$ in the stalagmite). Flowstone samples were prepared in the same way.

PREPARATION OF STANDARDS FOR TRACE ELEMENT ANALYSIS

Standards were prepared using the carbonates of the required metals. The carbonates were dissolved and diluted following a procedure similar to that for dissolving and diluting samples. The same sources of DDH_2O and HCl were used for all standards and samples.

The following stock solutions were prepared and stored:

80,000 ppm Ca prepared from Analar $CaCO_3$
80,000 ppm Ca prepared from Spex pure $CaCO_3$
100 ppm Ca prepared from Spex pure $CaCO_3$
100 ppm Sr prepared from Spex pure $SrCO_3$
100 ppm Mg prepared from Spex pure $MgCO_3$

Standards were prepared as required from these stock solutions. Standards prepared from Spex pure Ca stock were used to determine interference effects (of Ca on Mg and Sr signals). Standards prepared from Analar $CaCO_3$ stock were used in analyses of stalagmites. The Analar $CaCO_3$ contained 496±30 ppm Sr.

Initially four standards at 0.5, 1, 2.5 and 5 ppm Sr were used to analyse for Sr. A linear plot of [Sr] against A (absorbance) was obtained. In later work only the first three standards were used. Five standards at 0.1, 0.2, 0.5, 1 and 2 ppm Mg were used to analyse for Mg. The graph of A against [Mg] is linear to ∿0.5 ppm Mg.

APPENDIX II

ANALYSIS OF STALAGMITE SAMPLES USING ATOMIC ABSORPTION SPECTROPHOTOMETRY

Interference Effects

Magnesium

Calcium does not cause any change in the absorbance signal for Mg, in concentrations up to 4000 ppm Ca. Analyses for Mg were carried out using Ca free standards.

Strontium

Calcium causes a considerable decrease in the absorbance signal for Sr. An attempt was made to calibrate for this effect. Signal depression varies from about 5% at 500 ppm to about 20% at 2000 ppm Ca (see Calibration Chart P. 88). This effect was found to vary unpredictably by several per cent due to small changes in flame parameters. For this reason analysis of stalagmite was carried out with standards and samples at 1600 ppm Ca.

Ca Suppression Calibration Chart for Sr Analyses

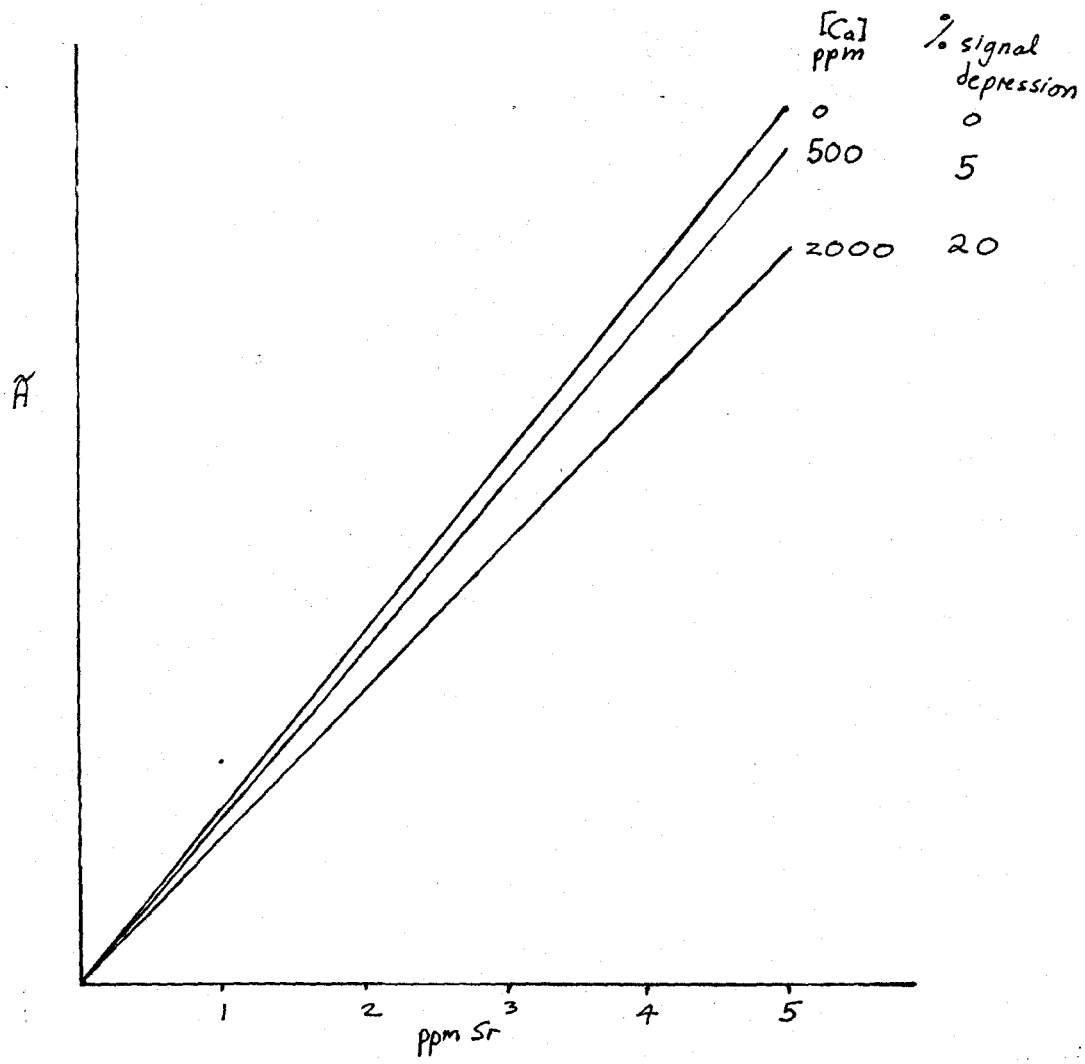

Procedure - Calculations

Analyses were carried out using a Perkin-Elmer atomic absorption spectrophotometer. An air acetylene flame and 3 slot burner were used.

Several absorbance readings were obtained for each sample and standard. Average values were obtained and used to calculate concentrations of Mg or Sr. Calculation of [Mg] and [Sr] were carried out using the programs POLYREG for Mg and LINREG for Sr.

APPENDIX III

DATA TABLES

SAMPLE NO. LOCATION

76108 Yorkshire, England. White Scar Cave

DATES: Top 5.6±0.4 Ka BP
Base 11.6±0.7 Ka BP

	#	cm from base	Age Ka BP	Mg ppm	Sr ppm	Mg:Sr		
	c	0.5	11.49	955	85	11.2		
A	11	1.7	11.21	1232	123	10.0		
	q	3.5	10.80	1181	138	8.5		
X	B	6.0	10.24	872	194	4.5		
	A	8.0	9.78	883	154	5.7		
I	7	10.8	9.14	1252	97	12.9		
	K	12.3	8.8	1110	154	7.2		
A	8	12.3	8.8	952	168	5.7		
	P	15.9	7.99	906	154	5.9		
L	J	18.3	7.44	618	223	2.8		
	O	20.2	7.01	745	183	4.1		
	Z	22.5	6.49	709	194	3.6		
	n	24.7	5.99	729	190	3.8		
	x	26.4	5.60	686	194	3.5		
	c	0.5	11.99	955	85	11.2	c	
O	12	2.5	11.21	1177	117	10.0	11	
B	9	4.25	10.8	1211	142	8.5	Q	correlation
L	1	5.5	10.24	995	142	7.0	B	with axial
I	2	6.6	9.78	1117	122	9.1	A	profile used
Q	3	7.4	8.82	1261	112	11.2		to estimate
U	4	8.6	7.39	1105	132	8.4		ages
E	5	9.4	6.44	1172	112	10.5	x	
	6	10.1	5.6	1142	107	10.7		
	S	descending		1100	114	9.6		
	U	one growth		1089	125	8.7		
	G	layer		1145	114	10.0		
	e	descending		1209	130	9.3		
	d	one growth		1258	130	9.8		
	f	layer		1217	102	11.9		

SAMPLE NO. LOCATION

76129 Yorkshire, England, Easegill Caverns

DATES: Top 0.5±0.8 Ka
Base 9.7±1.0 Ka

	#	cm from base	Age Ka BP	Mg ppm	Sr ppm	Mg:Sr		
	1	1.3	9.3		157	11.1		
A	2	4.0	8.5		145	7.3		
	g	6.5	7.8	1432				
X	f	8.9	7.1	1328				
	e	10.9	6.5	1464				
I	3	12.8	5.9		169	10.7		
	4	14.4	5.4		181	11.3		
A	5	17.2	4.6		194	9.9		
	d	19.1	4.0	1526				
L	c	21.3	3.4	1616				
	6	23.4	2.8		181	9.6		
	b	26.1	2.0	1574				
	a	29.4	1.0	1487				
O								
B	1	1.3	9.3		157		1	correlation with axial profile used to estimate ages
L	7	2.4	7.8		145			
I	8	3.3	6.5		145			
Q	10	5.3	3.8		146			
U	11	6.4	2.24		206			
E	12	7.3	1.0		230		a	

89

SAMPLE NO. 76130

LOCATION: Yorkshire, England. Easegill Caverns

DATES; Top 5.5±0.2
Base 10.1±0.5, 9.6±0.3 two determinations

	#	cm from base	Age Ka BP	Sr ppm	
	1	1.2	9.9	332	
	2	2.7	9.6	393	
	3	5.7	9.0	282	
	4	8.0	8.6	344	
	5	9.0	8.4	344	
	6	9.75	8.3	369	
A	7	11.2	8.0	258	
X	8	12.2	7.8	196	
I	9	13	7.7	233	
A	10	15.1	7.3	294	
L	11	16.5	7.0	320	
	12	17.4	6.9	270	
	13	19	6.6	270	
	14	21.25	6.2	282	
	15	22.75	5.9	295	
	16	24.5	5.6	332	
	17	2.5	9.6	381	1) Correlation with axial profile used to estimate ages
	18	3.75	9.0	356	4)
	19	4.75	8.5	356	
	20	5.4	8.4	336	
O	21	7.25	8.1	328	
B	22	8.25	8.0	356	
L	23	9.1	7.8	356	
I	24	9.9	7.75	344	9)
Q	25	10.9	7.6	344	
U	26	12.2	6.5	337	
E	27	13.4	6.35	289	
	28	14.2	5.9	344	
	29	14.9	5.6	336	16)

76144

Sample #	Mg ppm
1	1212
2	1250
3	937
4	1087
5	1062
6	1025
7	937
8	800
9	812
10	862
11	1025
12	1125
13	600
14	1250
15	1350
16	1212
17	1000
18	887
19	712
20	775
21	750
22	950
23	800
24	787
25	675
26	900
27	462

[Sr] ≈ 35 ppm (∿ constant). Single determination of Mg (26/8/78).

SAMPLE NO.
76190

LOCATION
Yorkshire, England. Gavel Pot

DATES:

Top 5.1±0.6 Ka BP
Base 14.7±0.6 Ka BP

#	cm from base	Age, Ka BP	Mg ppm	Sr ppm	Mg:Sr
g	4.8	14.12	538	135	4.0
h	5.5	14.40	420	117	3.6
i	7.0	13.85	397	137	2.9
j	7.7	13.80	357	122	2.9
k	13.3	13.10	380	152	2.5
q	21.3	12.13	340	194	1.7
r	23.2	11.91	337	209	1.6
s	26.4	11.52	349	134	2.6
t	30.1	11.08	346	136	2.5
u	32.5	10.79	390	147	2.6
v	36.7	10.30	294	149	2.0
w	40.6	9.81	353	132	2.7
x	42.3	9.60	341	122	2.8
y	44.5	9.34	409	123	3.3
z	52.5	8.02	422	107	3.9
A	55.0	7.90	383	109	3.5
B	56.5	8.80	376	120	3.1
ℓ	60.0	7.48	284	182	1.6
m	61.25	7.33	273	182	1.5
n	62.5	7.18	284	162	1.7
o	66.25	6.72	348	175	2.0
p	67.5	6.57	344	153	2.2
c	69.5	6.33	388	135	3.0
f	73.0	5.91	299	202	1.5
b	75.5	5.61	366	220	1.7
e	78.0	5.31	388	135	2.9
a	79.75	5.1	372	210	1.8
B	descending)		376	120	3.1
C	one)		475	125	3.8
D	growth)	8.8	419	112	3.7
E	layer)		414	120	3.4
F	)		473	118	4.0
	descending)				
A	one)	7.9	383	108	3.5
H	growth)		450	-	-
	layer)				

SAMPLE NO. LOCATION

76191 Yorkshire, England. Gaping Gill

DATES: Top 0.9±0.1 Ka BP
Base 11.4±0.6 Ka BP

	#	cm from base	Age, Ka BP	Mg ppm	Sr ppm	Mg:Sr
A						
X	1	0.75	11.1	448	188	2.4
I	2	1.9	10.7	452	165	2.7
A	3	2.75	10.4	431	141	3.1
L	4	3.9	10.3	390	141	2.8
	5	4.75	9.7	355	173	2.1
	6	6	9.3	354	165	2.1
	7	6.75	9.0	370	212	1.7
	8	7.9	8.6	327	188	1.7
	9	9.25	8.1	379	166	2.3
	12	13.5	6.7	328	154	2.1
	13	16	5.8	316	184	1.7

SAMPLE NO. LOCATION

76208 Yorkshire, England. Gaping Gill

DATES: Top 0.7±0.5
Base 2.9±0.4

#	cm from base	Ka BP	Mg ppm	Sr ppm	Mg:Sr		
l	1	2.81	798	228	3.5		
13	2.4	2.70	743	236	3.1		
m	3.8	2.58	805	250	3.2		
ℓ	5.4	2.44	975	262	3.7		
16	6.25	2.37	1002	236	4.2		
14	8.2	2.21	804	205	3.9		
15	10.5	2.01	812	242	3.4		
k	12.4	1.85	852	283	3.0		
17	14.9	1.64	758	157	4.8		
j	16.7	1.49	782	240	3.3		
18	18.7	1.32	789	187	4.2		
19	21.75	1.06	742	151	4.9		
i	23	0.96	742	294	2.5		
h	25.2	0.77	776	327	2.4		
20	26.05	0.70	703	224	3.1		
1	1	2.81	798	228	3.5	1)	
2	1.7	2.75	877	234	3.7	13)	correlation
3	2.4	2.70	817	246	3.3	)	with
4	3.2	2.65	834	212	3.9	)	axial
5	4	2.6	869	216	4.0	m)	profile
6	4.7	2.5	964	175	5.5	)	used
7	5.5	2.4	962	175	5.5	L)	to
8	6	2.1	943	187	5.0	)	estimate
9	6.75	1.7	899	158	5.7	18)	ages
10	7.5	1.3	818	170	4.8	)	

SAMPLE NO. 77143*

LOCATION Yorkshire, England, Ingleborough Cave

DATES: Top 125 Ka BP
Base 195 Ka BP

#	cm from base	Age Ka BP	Mg ppm	Sr ppm	Mg:Sr	$\delta^{13}C_{PDB}$	$\delta^{18}O_{PDB}$
1	8.8	129	490	35	14	-10.767	-4.182
2	8.4	132	592	30	20	-11.252	-4.288
3	8.1	135	424	36	12	-11.463	-4.166
4	7.7	138	391	32	12	-11.411	-4.424
5	7.3	141	436	34	13	-11.006	-4.189
6	6.8	144	504	31	16	-11.315	-4.388
7A	6.4	147	530	31	17	-10.865	-4.414
7B	5.9	151	659	25	26	-10.743	-4.138
8	5.2	156	595	15	40	-10.649	-4.133
9	4.7	160	537	25	21	-10.917	-4.228
10	4.3	163	558	25	22	-10.944	-4.088
11	3.7	167	509	25	20	-	-
12	3.3	170	493	25	20	-10.198	-4.302
13	2.8	174	593	17.5	31	- 9.755	-3.903
14	2.2	178	549	25	22	-	-
15	1.8	182	559	15	37	- 9.693	-4.000
16	1.2	187.6	549	15	37	- 9.862	-3.939
17	1.0	187.8	480	13.5	36	- 9.865	-3.865
18	0.7	192	517	20	26	- 9.681	-3.946
19	0.4	195	508	25	20	- 9.572	-3.844
20	0		541	23	24	- 9.777	-3.715

*Data provided by M. Gascoyne

SAMPLE NO. LOCATION

76008 Vancouver Island, Cascade Cave

#	cm from base	Mg ppm	Sr ppm	Mg:Sr
a	4.1	1063	28	38
b		1052	28	37
c		1056	28	37
d		1019	28	36
e	8.6	743	41	18
g		728	33	22
f		792	33	24
h		805	33	24
i	7.2	589	45	13
j	1.6	705	45	16

SAMPLE NO. LOCATION

75123* Vancouver Island. Cascade Cave

DATES: Top 50.5±6.9 Ka
Base 56.1±3.7 Ka

#	cm from base	Age Ka BP	Mg ppm	Sr ppm	Mg:Sr
1	0.3	56.4	1192	48	24.8
2	1.0	55.8	1090	60	18.1
3	1.4	55.5	955	54	17.6
4	2.0	54.9	972	60	16.2
5	2.5	54.5	1297	57	22.7
6	2.9	54.1	1082	54	20.0
7	3.4	53.7	1150	60	19.2
8	4.1	53.0	1560	48	32.5
9	4.9	52.4	1360	63	21.6
10	5.6	51.75	1045	54	19.4
11	6.0	51.4	1002	60	16.7
12	6.7	50.8	955	87	11.0

*Samples analysed in 1977.
[Ca] in solutions analysed for Sr was 4000 ppm.
Error for [Mg] and [Sr] determinations was estimated at <±10%.

SAMPLE NO. LOCATION

GV2 Grape Vine Cave, West Virginia

DATES: Top 12 cm, linear growth from 100-50 Ka BP
Base 2 cm, mean age 160 Ka BP

#	cm from base	Mg ppm	Sr ppm	$\delta^{18}O$	$\delta^{13}C$	Mg:Sr
1	0.8	3425	127	-4.7	-2.5	27
2	1.8	2917	120	-4.87	-2.3	24
3	2.9	1837	96	-5.39	-5.7	19
4	3.7	1753	79	-6.05	-5.7	22
5	4.6	1447	79	-6.9	-5.2	18
6	5.6	2311	127	-5.45	-4.35	18
7	6.4	1656	95	-5.3	-4.6	17
8	7.3	2192	94	-4.51	-4.1	28
9	8.2	2053	78	-5.75	-4.85	26
10	9.8	2269	110	-4.2	-4.7	21
11	10.8	1839	66	-4.55	-5.25	28
12	12.1	1436	63	-4.2	-4.3	23
13	13.0	1420	90	-4.6	-3.5	16
14	13.9	1286	62	-4.8	-3.5	21

$\delta^{18}O$ and $\delta^{13}C$ interpolated from Thompson's (1973) data

SAMPLE NO. GV2 Thompson's (1973) Data*

Distance from base of flow-stone, cm	$\delta^{18}O°/_{oo}$ PDB	$\delta^{13}C°/_{oo}$ PDB	Age, Ka BP
17	-4.52	-2.8	60.4±2.9
16.6	-5.05	-3.8	
16.1	-4.45	-3.1	
15.9	-4.05	-3.4	81.2±6.6
14.7	-4.25	-4.3	
14	-4.35	-4.0	70±3.6
13.3	-4.68	-5.2	
12.6	-4.2	-5.6	69±2.8
11.9	-4.2	-4.7	
11.1	-4.15	-4.9	
10.5	-4.75	-4.8	85.9±3.0
9.55	-4.72	-4.9	
8.8	-4.51	-4.1	79.5±2.1
8.1	-5.65	-5.1	
7.6	-5.15	-4.3	
7.2	-5.1	-5.0	
6.6	-5.6	-4.1	97.2±2.5
6	-7.0	-5.7	
5.25	-6.8	-4.7	
4.7	-6.3	-6.0	105.5±2.7
4.2	-5.3	-5.3	
3.5	-5.39	-5.7	9.6±3.9
3	-4.2	-3.2	
2.3	-4.85	-2.2	
1.65	-5.0	-2.6	156.0±6.9
1	-4.7	-2.5	
0.5	-4.35	-2.3	

*corrections to isotope data listed in 1973 Ph.D. thesis (Thompson, 1973) provided by Schwarcz (1978).

APPENDIX IV

ACCURACY AND PRECISION OF RESULTS

RESULTS OF REPEAT DETERMINATIONS

RESULTS OF ANALYSES OF STANDARDS

ERROR CALCULATIONS

Standard samples - Mg analyses

[Mg] ppm in solution	[Mg] ppm in 'stalagmite'	Dilution	Date
0.5228	653	1	30/5/78
0.5092	636	1	31/5/78
0.5016	627	2	30/5/78
0.5074	634	2	30/5/78
0.5074	634	2	31/5/78
0.5141	643	3	31/5/78
0.4818	602	3	1/5/78
0.5088	636	4	7/6/78
0.4961	620	4	29/6/78
0.4955	619	5	7/6/78
0.5025	628	5	29/6/78
0.5087	636	6	3/7/78
0.4884	610	6	4/7/78
0.4942	618	7	7/7/78
0.5161	645	7	18/7/78
0.4820	602	9	1/4/79
0.4820	602	9	1/4/79

Samples diluted to 320 ppm Ca from a stock standard solution at 1600 ppm Ca.

$$\sigma^2 \simeq s^2 \equiv \frac{1}{N-1} \Sigma (x_i - \bar{x})^2 = \frac{1}{16} \Sigma (x_i - 625.6)^2$$

$$\sigma = 16 \ (2.5\%)$$

Standard samples - Sr analyses

Date	[Sr]*ppm
1/4/7	1.86
1/4/79	1.89
1/4/79	1.96
15/1/79	1.96
15/1/79	1.86
15/1/79	1.89
8/1/79	2.00
8/1/79	1.93
8/1/79	1.97
29/12/78	1.9
29/12/78	1.99
1/8/78	1.95
1/8/78	1.97
17/7/78	1.97
7/7/78	1.99
4/7/78	2.00
3/7/78	1.97
3/7/78	1.99
3/7/78	1.94
3/7/78	1.96
8/6/78	1.97
7/6/78	1.99

*[Sr] in 1600 ppm Ca solution prepared from analar $CaCO_3$, computed from intercept of Sr calibration curve

$$\sigma^2 = \frac{1}{22} \Sigma(x_i - 1.95)^2$$

$$\sigma = .041833 \ (2.1\%)$$

Precision of Results

Sr

In cases where a regression error of >2% was obtained for the calibration curve were discarded. Repeat determinations of the Sr concentration in standard solution yield a σ of 0.04 ppm. An error of 0.04 ppm would give an error of 10 ppm in the result calculated for $[Sr]_s$. Minimum sensitivity obtained was 0.1 ppm in solution - giving a maximum error of 25 ppm $[Sr]_s$.

Mg

Repeat determinations of Mg in stock standard solutions gave a σ of $\pm$16 ppm $[Mg]_s$ (2.5% of the mean value in this case).

Repeat determinations were made for most samples. Reproducibility is not as good in the range where the Mg calibration curve is non-linear but determination of Mg in this range avoids additional errors involved in diluting samples.

Reproducibility was within 20 ppm for speleothem with <1250 ppm Mg in solution. Above this level repeat determinations show a larger variation - the largest difference was 126 ppm in samples with <2000 ppm Mg and 257

in a sample with ∿3000 ppm Mg. In these cases relative values remained the same for different determinations - all samples being analysed at one time. Precision is always better than ± 10%.

Weighing

Weighing errors cause comparable error in determination of [Mg] and [Sr] but do not affect Mg:Sr ratio.

Analysis of Interlaboratory Limestone Standard ZGI

An 0.1 g aliquot of the interlaboratory limestone standard ZGI was weighed, dissolved in HCl and diluted to 1600 ppm Ca as for stalagmite samples. An insoluble residue was removed by filtration before diluting the dissolved limestone.

The solution contained 1345 ppm Ca after dilution (assuming the entire soluble fraction consisted of $CaCO_3$). Analysis for Sr using standards containing 1600 ppm Ca and correction of the result using Ca suppression calibration chart gave a value of 512 ppm Sr. The recommended value of [Sr] for this sample is 490 ppm. Our value is 4.4% higher.

Analysis for Mg gave results of approximately 2000 ppm Mg. The recommended value for Mg in this standard is 7200 ppm.

A second 0.1 g aliquot was weighed and dissolved using 3 ml HCl and 3 ml 48% HF. When analysed for Mg this sample gave a value of 5620 ppm Mg. The low result obtained is probably due to Si interference. (This sample gave consistently low values for Sr.) A calcite standard should be analysed - or analyses of ZGI for Mg should be made after dissolving the sample and removing the Si.

Repeated Weighings

Weights in grams			Difference
2.93088	2.93086		0.00002
2.94045	2.94030		0.00015
2.96315	2.96309		0.00011
2.96273	2.96290		0.00007
2.85445	2.85440		0.00005
2.94712	2.94722		0.00010
2.85637	2.85644		0.00007
2.92263	2.92285		0.00022
2.97820	2.97881		0.00061
2.85691	2.85742		0.00059
2.98024	2.98024		0.00000
5.09570	5.09575	5.09570	0.00020
2.72781	2.72795	2.72780	0.00015

Maximum difference 0.0006 g. Maximum loss of precision due to weighing error 0.6% (samples weigh 0.1 g).

Analysis of ZGI limestone standard

Date	Sr, ppm	Sample #
6/4/79	528	1
6/4/79	520	2

	Mg, ppm	
1/4/79	5618	3
1/4/79	5616	3
3/2/79	2494	1
3/2/79	2706	2

Weight of Residue g	Weight of sample in solution g	ppm Ca in solution	
0.01475	0.08537	1366	1
0.01725	0.08279	1325	2
	0.1	∿1345	3

Samples 1 and 2 dissolved in HCl

Sample 3 dissolved in HF

76129

Sample #	Date 12/12/78	8/1/79
	Sr ppm	
1	147	168
2	147	144
3	172	168
4	172	192
5	196	192
6	172	192
7	147	144
8	147	144
10	147	144
11	196	216
12	221	240

	29/5/78	30/5/78	31/5/78	1/6/78
	Mg ppm			
a	1485	1521	1470	1472
b	1561	1587	1568	1581
c	1605	1635	1610	1616
d	1518	1540	1526	1520
e	1475	1474	1456	1452
f	1326	1343	1312	1330
g	1440	1446	1397	1445

*[Mg] > 2500 ppm, offscale on calibration curve

76130	Sr ppm	
Date:	29/12/78	8/1/79
Sample #		
1	327	337
2	402	385
3	276	289
4	352	337
5	352	337
6	377	361
7	252	264
8	176	216
9	226	240
10	276	313
11	327	313
12	276	264
13	276	264
14	276	289
15	301	289
16	327	337
17	377	385
18	352	361
19	352	361
20		337
21		337
22		361
23		361
24		337
25		337
26		337
27		289
28		337
29		337

*[Mg] > 2500 ppm, offscale on calibration curve

76190	Mg				Sr
Date (1978):	1/6	31/5	30/5	12/5	11/5*
a	343	385	375	387	210
b	337	386	375	386	220
c	362	415			135
e	362	415	392	406	140
f	275	320	302	319	202
g	514	546	541	552	135
h	343	386	367	117	
i	374	409	392	415	137
j	343	371	359	354	122
k	362	395	383		152
ℓ	269	298	286		182
m	257	292	269		182
n	269	298	285		162
o	300	341	318		175
p	324	365	342		153
q	324	353	342		194
r	311	359	342		209
s	326	371	349		134
t	319	371	349		136
u	373	407	390		147
v	265	317	300		149
w	326	377	357		132
x	311	365	349		122
y	395	425	407		123
z	402	443	423		107
A	365	401	382		109
B	350	395	382		120
C	458	485	465	492	125
D	402	437	415		112
E	395	431	415		120
F	482	464	474		118
H	451		449		

*No Ca in standards results corrected for Ca suppression - absolute values in error by ±5%. Relative values within previously stated error limits.

76191	Mg ppm		Sr ppm		
Date:	11/11/78	1/1/79	29/12/78	15/1/79	8/1/79
1	448		196	182	187
2	452		172	159	164
3	431		147	136	141
4	390		147	136	141
5	355		172	182	164
6	354		172	159	164
7	365	375	220	204	211
8	324	330	196	182	187
9		379	147		186
12		328	147		162
13		316	220		162

76108	Mg ppm										Sr ppm				
Date (1978):	29/5	30/5	31/5	1/6	7/6	29/6	3/7	4/7	7/7	18/7	7/6	3/7	4/7	7/7	17/7
Sample #															
a					893	873					154	154			
b					879	866					196	193			
c					947	963					84	87			
d					1260	1257					126	135			
e					1208	1211					126	135			
f					1216	1219					98	106			
g					1139	1151					112	116			
J					616	620					224	222			
K					1100	1121					154	155			
x					694	679					196	193			
z					707	712					196	202			
u					1079	1099					126	125			
n	732	750	715	735		715					196	185			
q	1205	1213	1158	1171		1158					140	136			
p	913	939	892	898		892					154	155			
o	750	768	734	741		734					182	185			
s					1093	1107					112	117			
1							1004	987				142	143		
2							1120	1114				123	121		
3							1270	1252				114	110		
4							1113	1097				133	132		
5							1187	1158				114	110		
6							1143	1141				104	110		
7							1255	1249				95	99		
8							961	944				171	165		
9							1223	1199				142	143		
11									1215	1250				118	128
12									1174	1180				118	116

76208	Mg ppm						Sr ppm		
Date (1978):	30/5	29/5	1/6	31/5	7/7	18/7	7/7	17/8	18/7
h	795	760	796	753					
i	759	732	757	721					
j	795	779	802	753					
k	867	846	867	829					
ℓ	1002	972	985	944					
m	822	798	804	797					
1					785	812	224	232	
2					867	888	236	232	
3					806	829	248	244	
4					823	845	212	-	
5					867	871	224	209	
6						964	177	174	
7					950	974	177	174	
8					921	966	189	186	
9					883	916	153	163	
10					795	841	165	174	
13						743		232	240
14						804		197	215
15						812		232	253
16						1002		232	240
17						758		151	164
18						789		186	189
19						742		151	151
20						703		221	227

76008		Sr ppm		Mg ppm	
Date (1978)		8/6	3/7	7/6	29/6
3	a	28	29	1047	1079
	b	28	29	1040	1065
	c	28	29	1040	1072
	d	28	29	1008	1030
6	e	43	39	743	765
	f	28	39	780	805
	g	28	39	718	739
	h	28	39	799	811
1	i	43	48	576	602
5	j	43	48	699	712

GV2	Mg ppm		Sr ppm	
Date:	6/4/79	6/4/79	6/4/79	6/4/79
Sample #				
1	3392*	3459*	125	130
2	3046*	2789*	117	122
3	1892*	1782*	94	97
4	1811	1696	78	81
5	1490	1405	86	81
6	2341	2282	125	130
7	1650	1663	94	97
8	2250	2134	94	86
9	2073	2033	78	78
10	2265	2273	110	110
11	1874	1805	70	63
12	1442	1431	62	63
13	1442	1399	94	86
14	1295	1278	62	63

*samples diluted to 160 ppm Ca before analysis

APPENDIX V

COMPUTER PROGRAMS

POLYREG

SAMPLE INPUT

7			No. of points on calibration curve
2.5	139	)	
2.5	139	)	
1.0	92	)	Sr concentration followed by
1.0	92	)	absorbance for standard
1.0	92	)	solutions
1.0	92	)	
0.5	75	)	
5			No. of sample Ã readings
10		)	
12		)	Ã for samples
15		)	
16		)	(Y values)
30		)	

PROGRAM LISTING

```
      PROGRAM POLYREG(INPUT,OUTPUT)
      EXTERNAL F
      DIMENSION XY(20,5),ALFA(2),IJOB(2),IND(9),VARB(15),ANOVA(16,5)
      DIMENSION XYB(5,5),WA(3),PAR(5)
      DIMENSION XSV(20)
      READ *,N
      READ *,((XY(I,1),XY(I,5)),I=1,N)
C PLOT THE ORIGINAL X,Y VALUES WITH *
      DO 7 I=1,N
      XSV(I)=XY(I,1)
7     CALL PLOTPT(XY(I,1),XY(I,5),4)
      DO 1 I=2,4
      DO 1 J=1,N
1     XY(J,I)=XY(J,1)**I
      PRINT601,((XY(I,J),J=1,5),I=1,N)
601   FORMAT("1MATRIX X IS ",/"0",20(5F10.4,/" "))
      M=4
      ALFA(1)=ALFA(2)=.05
      IJOB(1)=0
      IJOB(2)=2
      IND(1)=IND(2)=IND(3)=IND(4)=1
      IX=20
      IB=5
      CALL RLSEP(XY,N,M,IX,ALFA,IJOB,IND,ANOVA,XYB,IB,VARB,IER)
      PRINT 603,(XYB(I,1),I=1,5)
603   FORMAT(" MEANS",/"0",20(5F10.4,/" "))
      PRINT 605,((XYB(I,2),XYB(I,4),XYB(I,5)),I=1,4)
605   FORMAT(" COEFF",10X,"F-VALUE",3X,"PROB",5(/" ",F10.4,5X,F10.4,5X,
     +F10.4))
C PLOT THE YHAT VALUES WITH =
      DO 9 I=1,N
      YHAT=XYB(1,2)*XSV(I)+XYB(2,2)*XSV(I)**2+XYB(3,2)*XSV(I)**3
     ++XYB(4,2)*XSV(I)**4
9     CALL PLOTPT(XSV(I),YHAT,1)
C START INTERPOLATIONS
      READ *,NINT
      PRINT 607
607   FORMAT("0INTERPOLATIONS",/4X,"Y VALUE", 8X,"X VALUE",
     +8X,"X *1250",/" ")
      DO 3 I=1,4
3     PAR(I)=XYB(I,2)
      DO 5 KK=1,NINT
      READ *,PAR(5)
      EPS=1.0E-6
      NSIG=5
      N=1
      X=1.5
      ITMAX=100
      CALL ZSYSTM(F,EPS,NSIG,N,X,ITMAX,WA,PAR,IER)
C PLOT THEINTERPOLATED VALUES WITH +
      CALL PLOTPT(X,PAR(5),2)
      PRINT 609,PAR(5),X,X*1250.
609   FORMAT(" ",F10.4,5X,F10.4,5X,F10.4)
5     CONTINUE
      CALL OUTPLT
      PRINT 613
613   FORMAT(" ORIGINAL VALUES *, YHAT VALUES =, INTERPOLATED VALUES +")
```

SAMPLE OUTPUT

Y = A

X = ppm Mg in solution

X*1250 = ppm Mg in stalagmite

INTERPOLATIONS

Y VALUE	X VALUE	X *1250
79.0000	.5231	653.8921
174.0000	1.2266	1533.2208
181.0000	1.2807	1600.8688
186.0000	1.3195	1649.3971
176.0000	1.2420	1552.5140
169.0000	1.1881	1485.1100
155.0000	1.0811	1351.3456
166.0000	1.1651	1456.3280
95.0000	.6368	796.0553
91.0000	.6082	760.2492
95.0000	.6368	796.0553
103.0000	.6945	868.1735
118.0000	.8041	1005.1131
98.0000	.6584	823.0217
90.0000	.6011	751.3247
92.0000	.6153	769.1846
111.0000	.7528	940.9385
141.0000	.9752	1219.0335

SAMPLE CALIBRATION CURVE

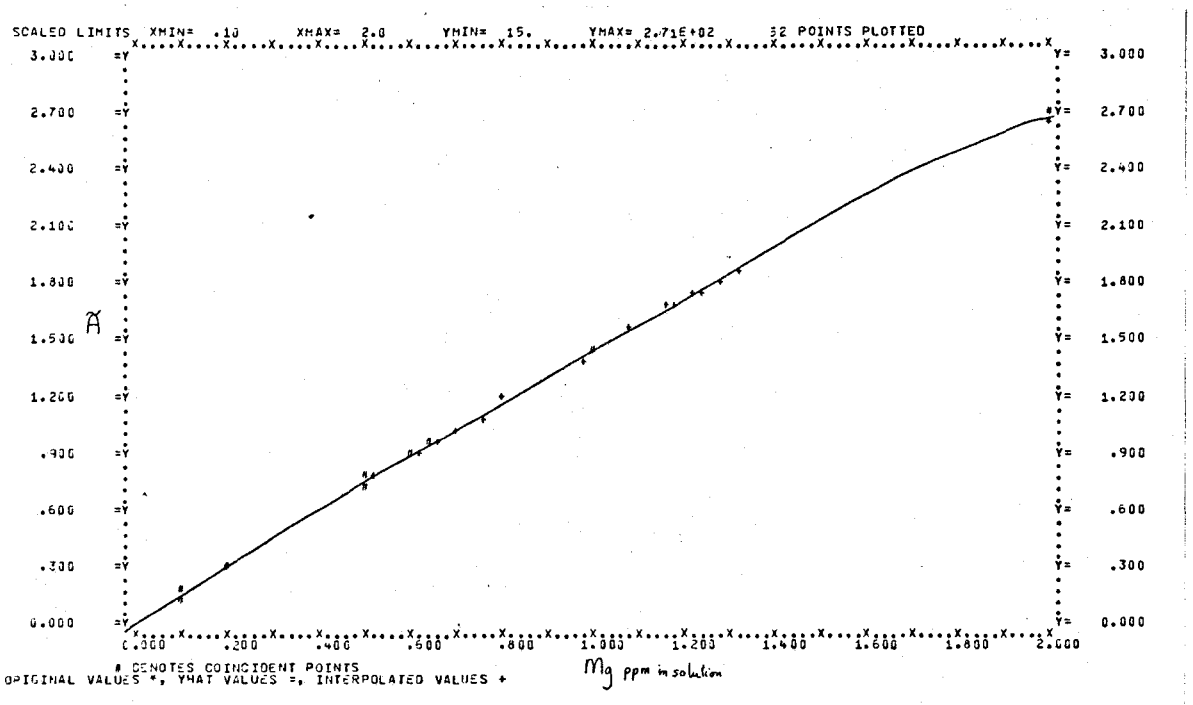

LINREG

SAMPLE INPUT

```
17 ———————————————— No. of points on calibration curve
0.1          15  )
0.1          15  )
0.2          31  )
0.2          30  )
0.2          30  )
0.2          31  )
0.5          73  )
0.5          75  )
0.5          75  )
0.5          76  )
1.0         142  )
1.0         142  )
1.0         146  )
2.0         266  )
2.0         271  )
2.0         271  )
2.0         270  )

18 ———————————————— No. of sample Ã readings
79                )
174               )
181               )
186               )
176               )
169               )
155               )
166               )      Ã for samples
95                )
91                )      (Y values)
95                )
103               )
118               )
98                )
90                )
92                )
111               )
141               )
```

PROGRAM LISTING

```
      PROGRAM LINREG(INPUT,OUTPUT)
      DIMENSION X(20,2),S(2,2),B(2,2),A(2,2),INCD(3)
      DIMENSION XMEAN(2),XSV(20)
      M=2
C M = NO. OF VARIABLES
C N= NO. OF OBSERVATIONS (UP TO 20)
      READ*,N
      READ*,((X(I,J),J=1,M),I=1,N)
      DO 3 I=1,N
      XSV(I)=X(I,1)
3     CALL PLOTPT(X(I,1),X(I,M),4)
      IX=20
      IBAS=2
      CALL BEMIRI(X,N,M,IX,XMEAN,B,A,S,IBAS,INCD,IER)
      PRINT 609,XMEAN,S(1,1),S(2,2)
609   FORMAT("1",15X,"X",14X,"Y",/"0MEAN",6X,2F10.4,/" STD.DEV.",2X,2F10
     +.4)
      DO 5 I=1,N
      YHAT=A(1,2)+B(1,2)*XSV(I)
5     CALL PLOTPT(XSV(I),YHAT,1)
      PRINT 603,A(1,2),B(1,2)
603   FORMAT("0REGRESSION EQUATION IS ",/" Y = ",F10.4," + ",F10.4,
     +" * X",/" ")
      PRINT 611,S(1,2)
611   FORMAT(" STANDARD ERROR OF REGRESSION COEFFICIENT ",F10.4)
      READ *,NINT
      PRINT 605
605   FORMAT("0INTERPOLATIONS",/4X,"Y VALUE", 8X,"X VALUE",
     +8X,"X * 250",/" ")
      DO 1 I=1,NINT
      READ*,Y
      XV=Y/B(1,2)
      CALL PLOTPT(XV,Y,2)
      PRINT 607,Y,XV,XV*250.
607   FORMAT(" ",F10.4,5X,F10.4,5X,F10.4)
1     CONTINUE
      CALL OUTPLT
      PRINT 613
613   FORMAT(" ORIGINAL VALUES *, YHAT VALUES =, INTERPOLATED VALUES +")
      STOP
      END
```

SAMPLE OUTPUT

	X	Y
MEAN	1.3571	103.0000
STD.DEV.	.8018	25.3640

REGRESSION EQUATION IS
Y = 60.0741 + 31.6296 * X

STANDARD ERROR OF REGRESSION COEFFICIENT .2479

INTERPOLATIONS

Y VALUE	X VALUE	X * 250
10.0000	.3162	79.0398
12.0000	.3794	94.8478
15.0000	.4742	118.5597
16.0000	.5059	126.4637
30.0000	.9485	237.1194

Y = $\tilde{A}$
X = ppm Sr in solution
X*250 = ppm Sr in stalagmite

SAMPLE CALIBRATION CURVE

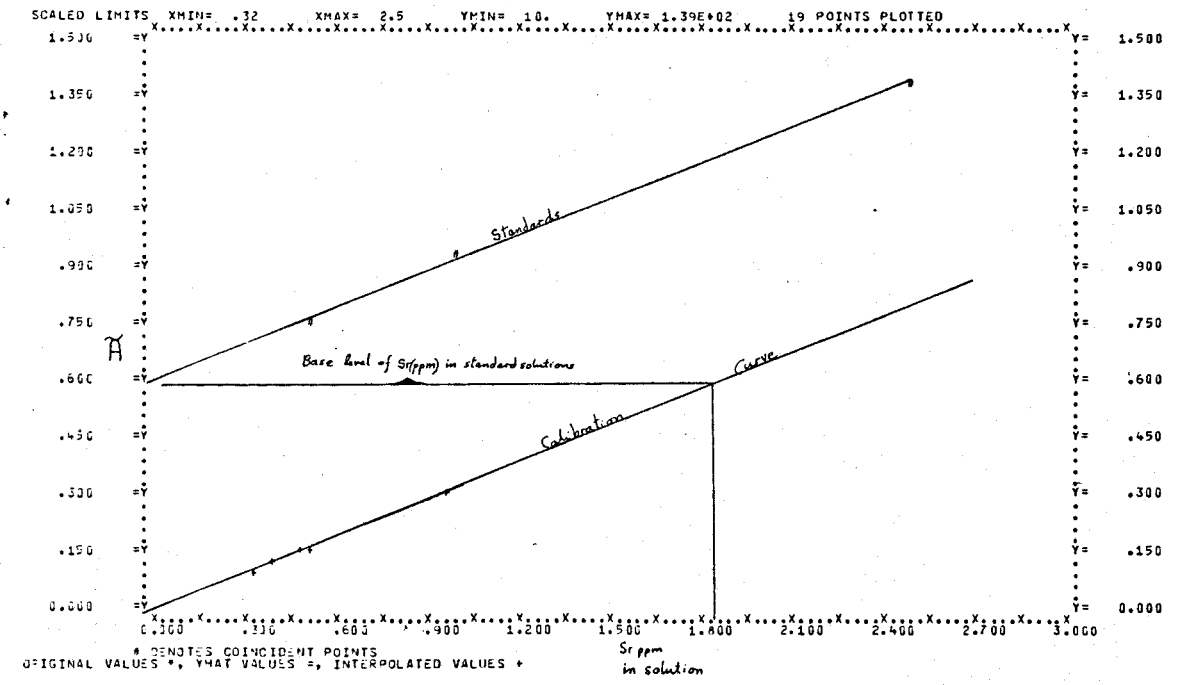

APPENDIX VI

RECORDS OF SAMPLE LOCATION, DATING AND COLLECTION

Sample Collection and Location

Records of collection sites are kept in the isotope dating laboratory at McMaster University. Maps of cave locations for English speleothem are given in the field guide by Glover (1971).

Dates

Dating was carried out in the isotope dating laboratories at McMaster University. Records of U and Th yields, concentrations and activities are filed there.

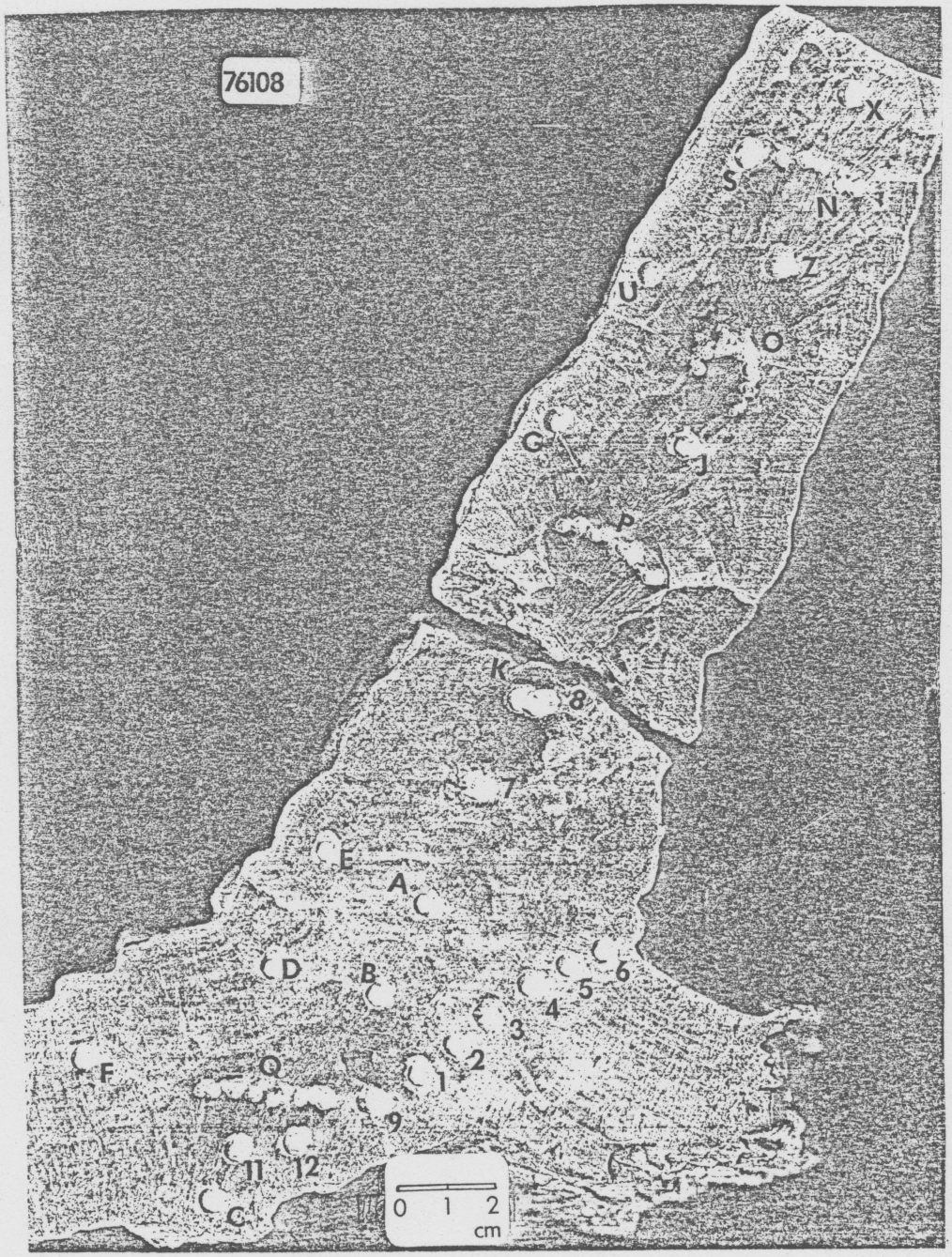
76108
X
S
N
Z
U
O
G
J
P
K
8
7
E
A
D
B
6
5
4
3
2
1
F
Q
9
11
12
C
0 1 2
cm

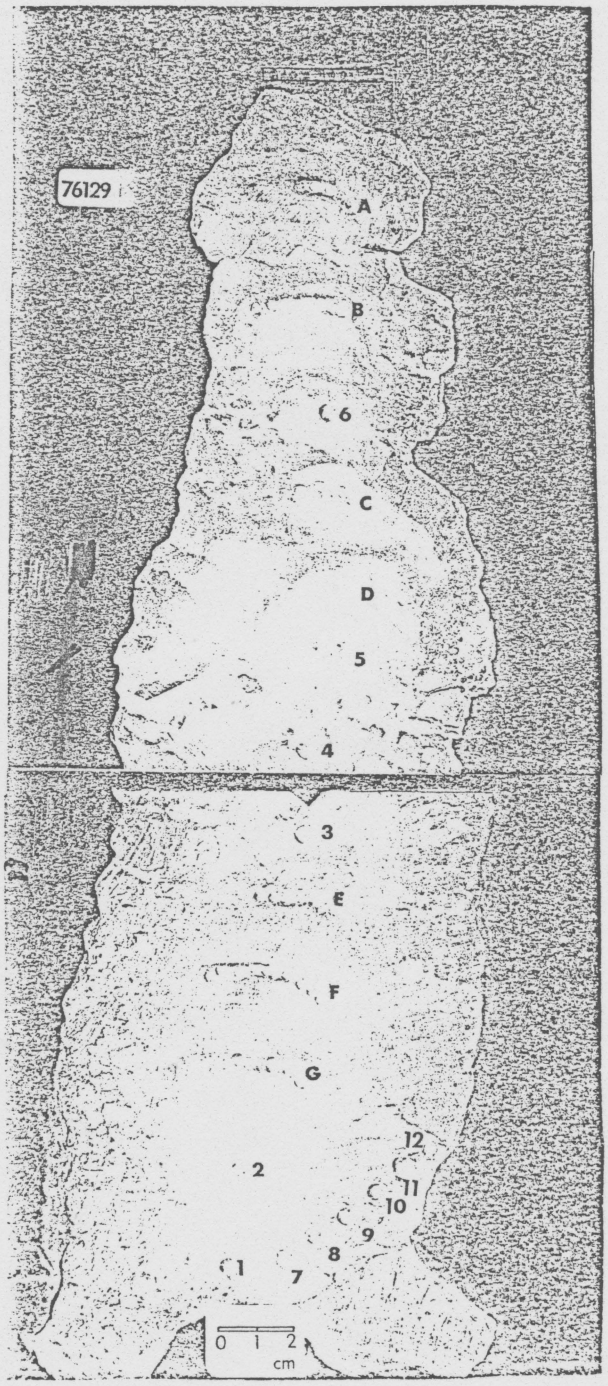
76129
A
B
6
C
D
5
4
3
E
F
G
12
2
11
10
9
8
1
7
0 1 2
cm

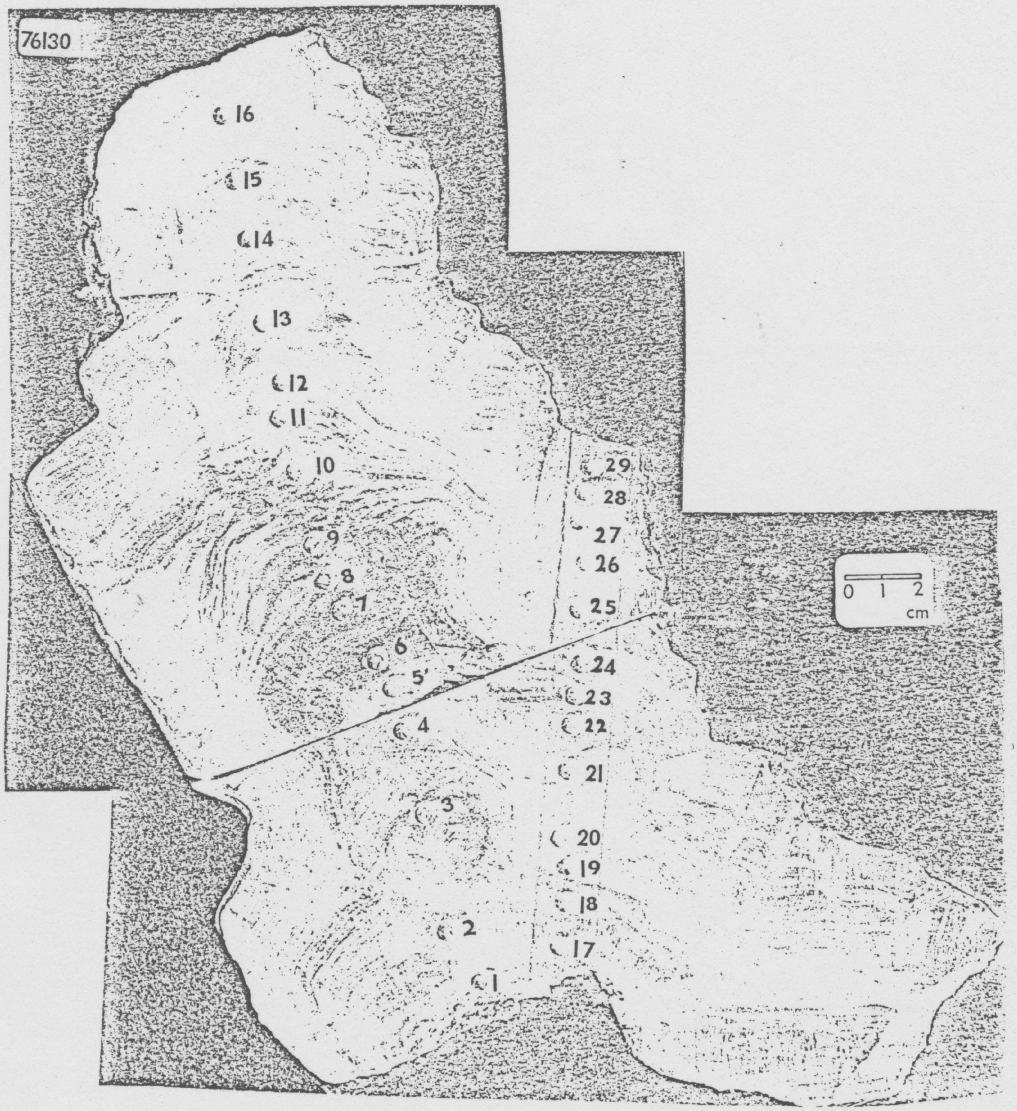
76130
16
15
14
13
12
11
10
9
8
7
6
5
4
3
2
1
29
28
27
26
25
24
23
22
21
20
19
18
17
0 1 2
cm

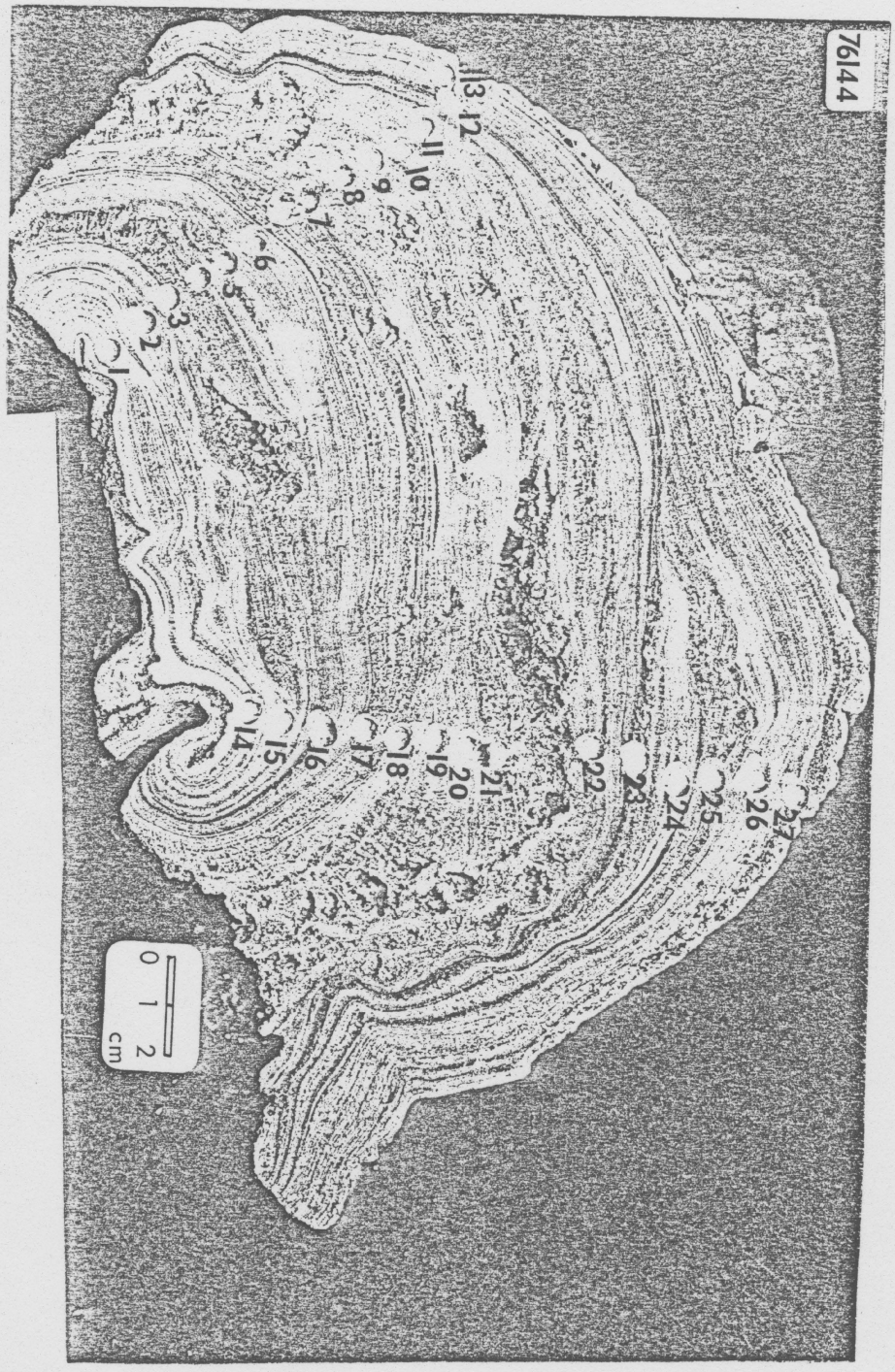
7644
1
2
3
5
6
7
8
9
10
11
12
13
14
15
16
17
18
19
20
21
22
23
24
25
26
27
0 1 2
cm

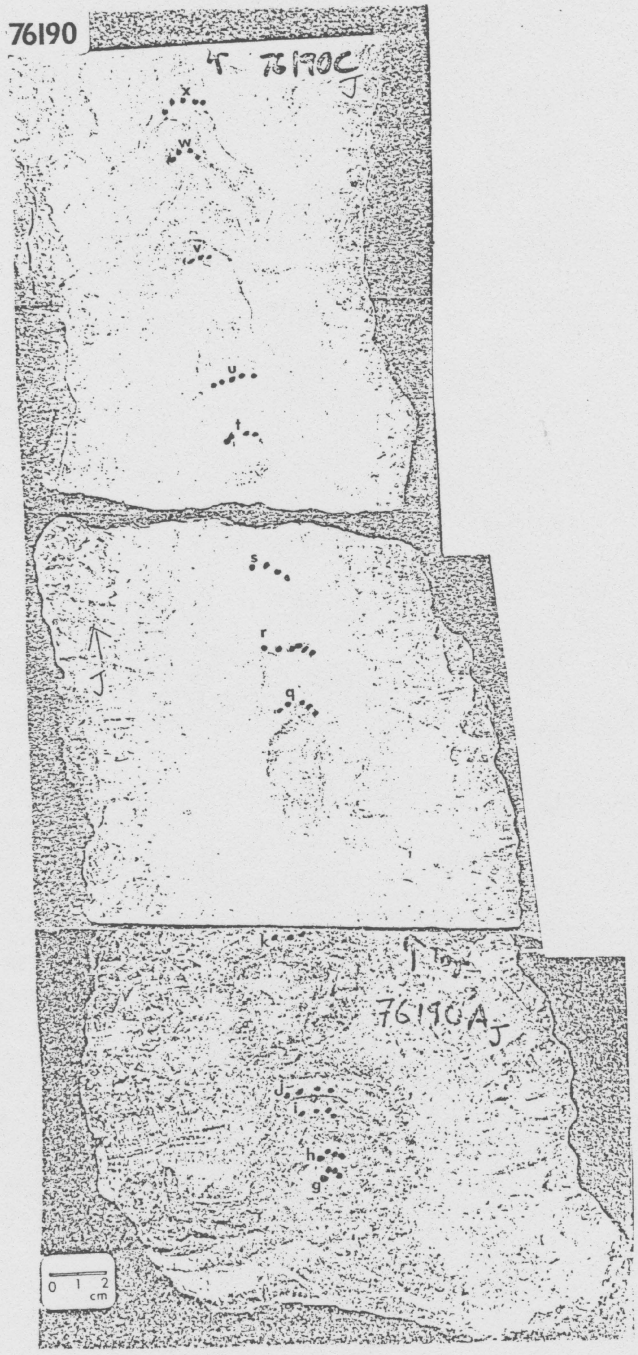
76190
T 76190C
J
x
w
v
u
t
s
r
q
J
k
Top
76190A
J
J
i
h
g
0 1 2
cm

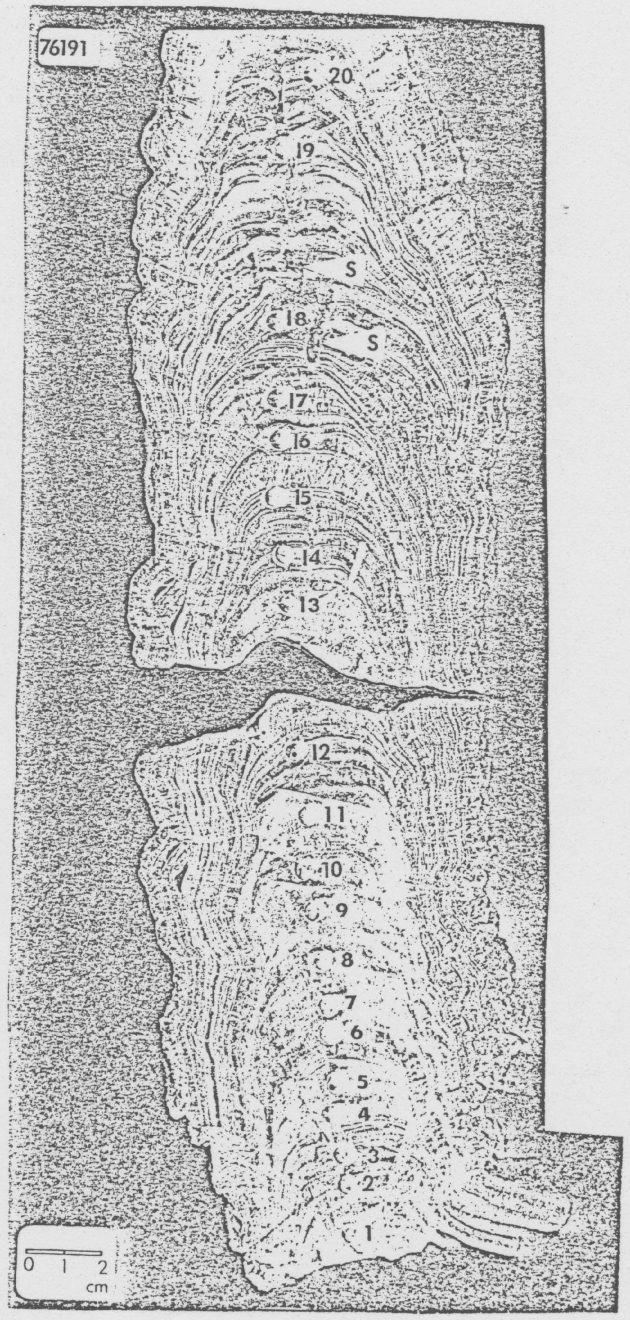

S = Pits (possibly solutional)

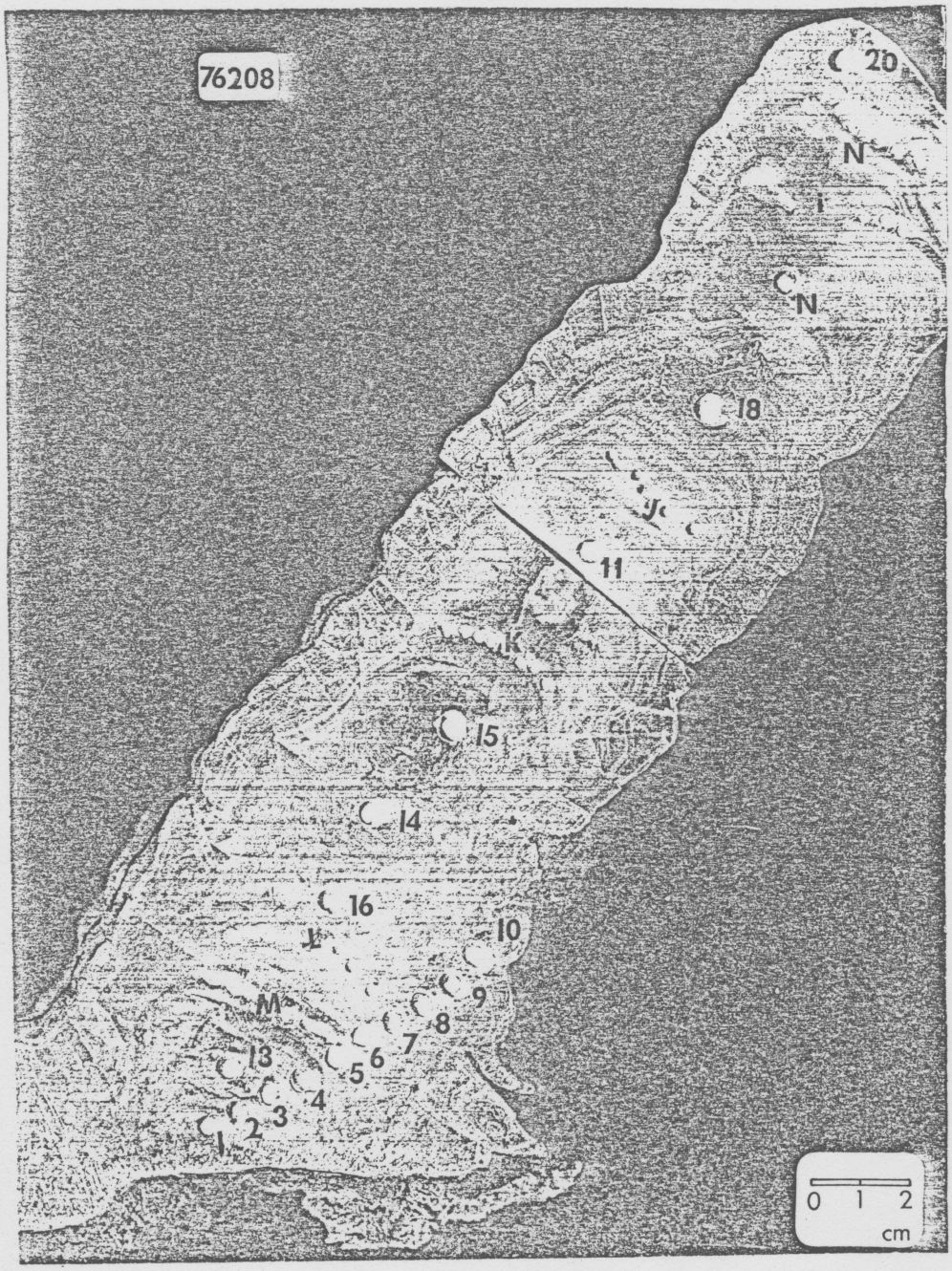
76208
20
N
N
18
11
K
15
14
16
10
9
M
8
7
6
5
13
4
3
2
1
0 1 2
cm

77143

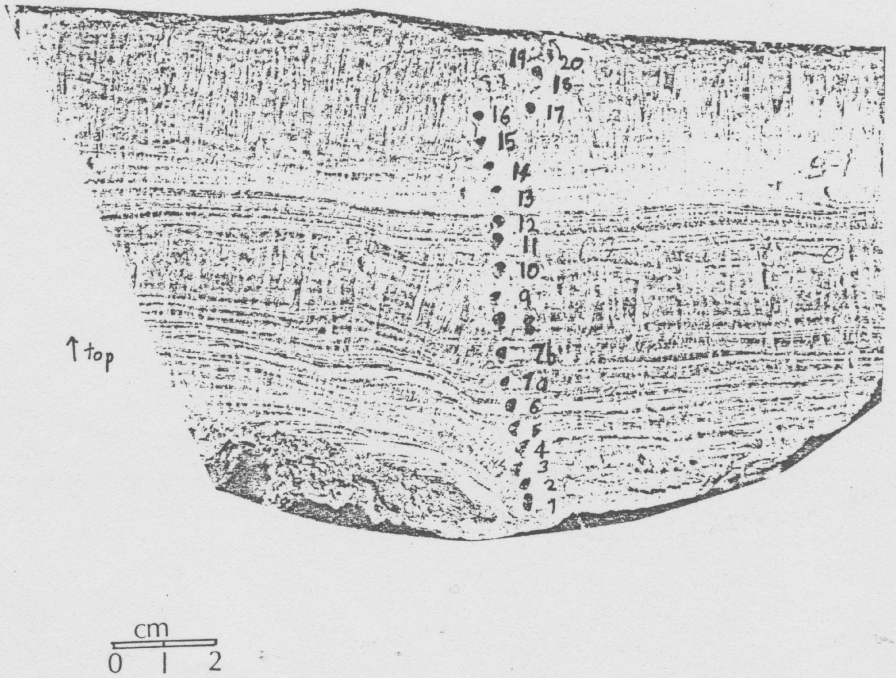

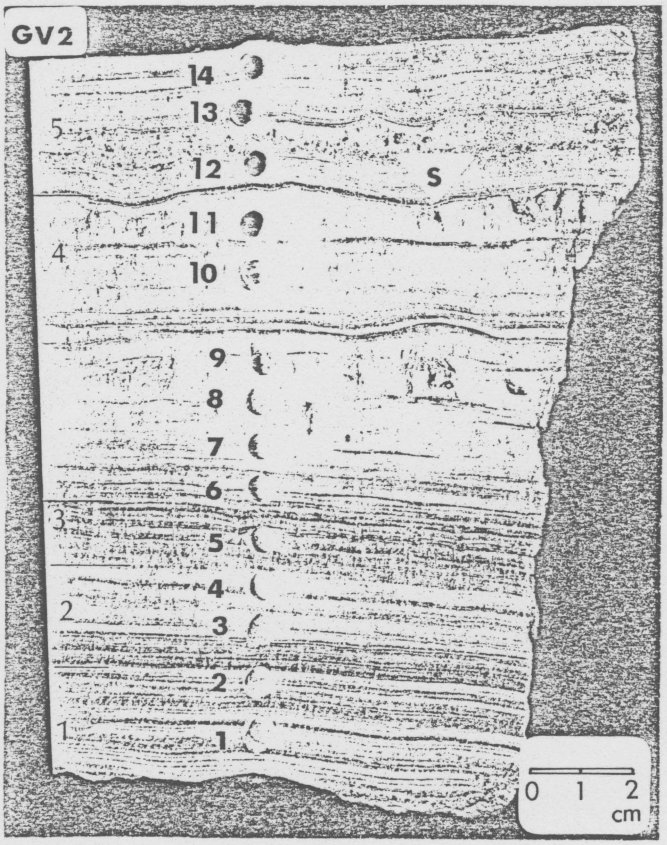

S = solution surface

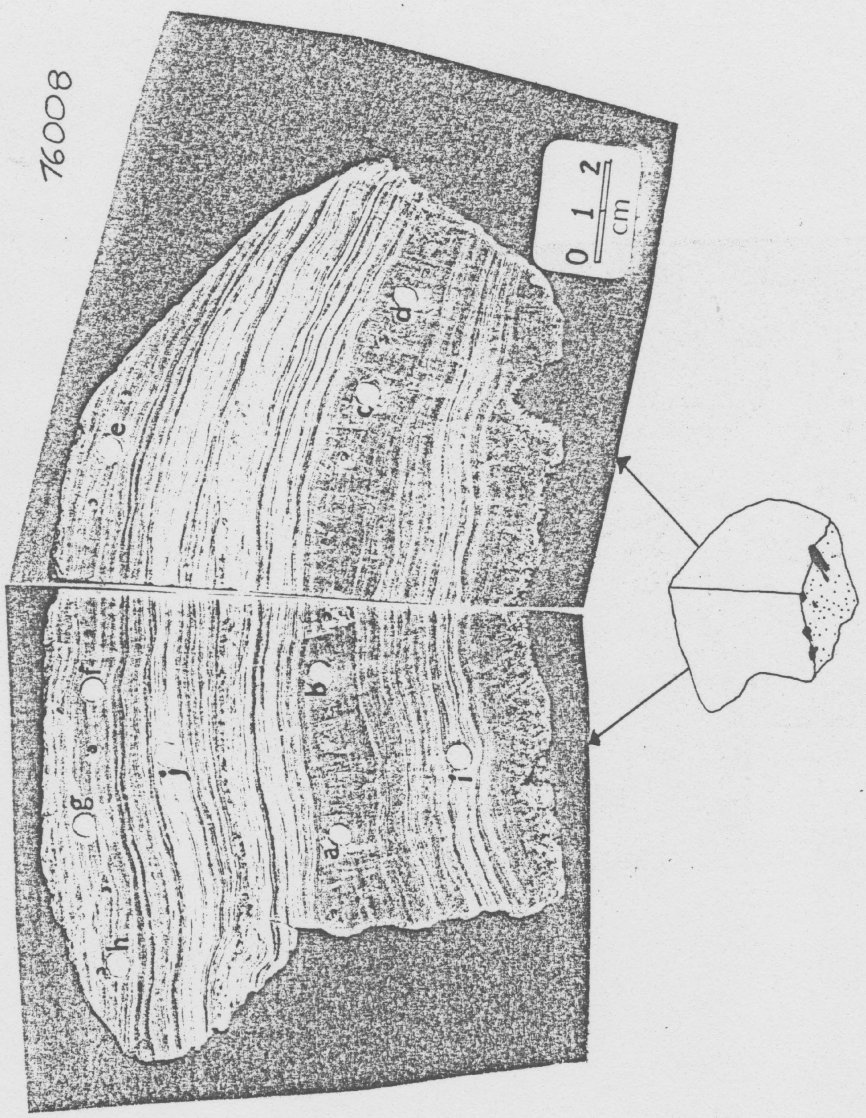
76008
0 1 2
cm

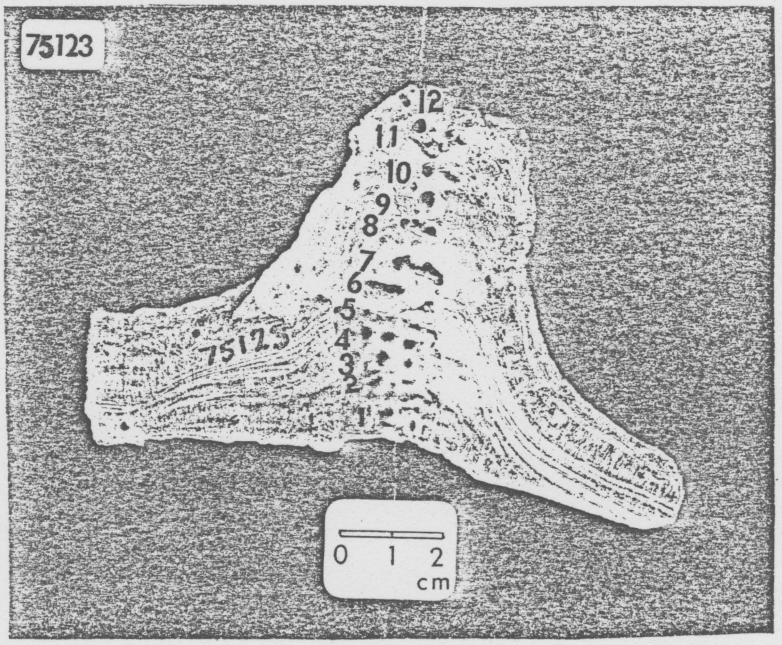
75123
12
11
10
9
8
7
6
5
4
3
2
1
75123
0 1 2
cm